

EXPERIMENTAL STUDY ON THE CHARACTERISTICS OF SOLAR
CELLS AND SOLAR CELL MODULES WITH RESPECT TO THE SOLAR
PROBE MISSION
PART II: SOLAR CELL MODULES

From: "Experimentalstudie über die Eigenschaften von Solarzellen und
Solarzellenmodulen im Hinblick auf die Mission einer Sonnensonde. Teil
II. Solarzellenmodulen", by Siemens AG in cooperation with Messerschmitt -
Boelkow GmbH; Contract RV4-SS/01/68; Period Covered: July 15, 1968 - Jan. 1,
1969; Messerschmitt - Boelkow Bericht nr. TSP-6.422.1; February 1969.

Translated by
Belov & Associates
for
N.A.S.A. GSFC Library
Contract NAS 5-10888
Item no. 10888-028
December 1969

FACILITY FORM 602

| | |
|-------------------------------|------------|
| N70-73727 | |
| (ACCESSION NUMBER) | (THRU) |
| 85 | None |
| (PAGES) | (CODE) |
| CR-110109 | |
| (NASA CR OR TMX OR AD NUMBER) | (CATEGORY) |



EXPERIMENTAL STUDY ON THE CHARACTERISTICS OF
SOLAR CELLS AND SOLAR CELL MODULES WITH RESPECT
TO THE SOLAR PROBE MISSION

PART II

Application Contract RV4 -SS/01/68

Report on Work from 7-15-68 to 1-31-69

Siemens Corporation in cooperation with the Messerschmitt-Bölkow Corp.

EXPERIMENTAL STUDY
ON THE CHARACTERISTICS OF SOLAR CELLS AND SOLAR CELL MODULES
WITH RESPECT TO THE SOLAR PROBE MISSION

Completed under contract from the Society for Space Research,
Ltd., under Contract No. RV4-SS/01/68

Part II Solar Cell Modules

Messerschmitt-Bölkow Report No. TSP-6.422.1

Main Project Department Space Flight System Studies

Director: D. E. Koelle

Project Engineer:

Grad. Eng. P. Kleber

Director of the Department:

Grad. Physicist Dr. E. Müller

Researcher:

Grad. Physicist J. Heinicke

Associates:

F. Köhler

J. Ohlich

Grad. Eng. L. Preuß

Engineer K.-P. Pühler

K.-H. Siegel

Dr. E. Suppa

TABLE OF CONTENTS

| | | |
|-----|--|------|
| 1. | <u>Introduction and Summary</u> | Page |
| 1.1 | Problem | 1 |
| 1.2 | Course of the Study | 2 |
| 1.3 | Summary of the Results | 3 |
| .31 | Cover Glass Assembly | 3 |
| .32 | Cell Connection | 3 |
| .33 | Base Foil | 4 |
| .34 | Complete Module | 4 |
| .35 | Module and Production Technique | 5 |
| 2. | <u>Cell Connection</u> | |
| 2.1 | Investigated Connection Techniques | 5 |
| 2.2 | Soft-Soldering | 6 |
| .21 | Selection of High-melting-point Solder | 6 |
| .22 | Soldering Process | 7 |
| .23 | Results | 8 |
| 2.3 | Hard soldering | 9 |
| .31 | Selection of low-melting point Hard-solder | 9 |
| .32 | Process | 10 |
| .33 | Results | 11 |
| 2.4 | Welding | 13 |
| .41 | General Comments | 13 |
| .42 | Welding Smooth Silver Foil | 13 |
| .43 | Welding Silver Foil by the Projection Welding Method | 16 |
| .44 | Welding Silver Mesh | 16 |
| .45 | Conclusions | 27 |
| 2.5 | Comparison of the Processes | 31 |
| 3. | <u>Cover Glass Assembly</u> | |
| 3.1 | Possibilities for Cover Glass Assembly | 33 |
| 3.2 | Optical Adhesives | 34 |
| .21 | Thermal Vacuum Process | 34 |
| .22 | Adhesion of Optical Adhesives at Various Temperatures | 34 |
| .23 | Transmission Changes of Optical Adhesives by U-V Radiation | 37 |
| .24 | Cover Glass Assembly | 42 |
| 3.3 | Non optical Adhesives | 45 |
| 3.4 | Cover Glass Assembly by Thermodiffusion | 48 |
| 3.5 | Losses through Non-optimal Index of Refraction Transitions between Cell and Cover Glass | 54 |

| | | |
|-----|--|----|
| 4. | <u>High Temperature Foils</u> | |
| 4.1 | Selection of Foil | 57 |
| 4.2 | Tests on Foil | 57 |
| 4.3 | Process for Fabrication of Modules | 59 |
| 4.4 | Conclusions | 60 |
| 5. | <u>Model Module</u> | |
| 5.1 | Module Construction (Production process) | 60 |
| 5.2 | Construction of Model Modules | 62 |
| 5.3 | Tests on Model Modules | 66 |
| .31 | Climate Test | 66 |
| .32 | Thermal Vacuum | 66 |
| .33 | Thermal Shock | 68 |
| .34 | Vibration | 68 |
| 6. | <u>Investigations on Thermal Balance</u> | |
| 6.1 | Test Module | 69 |
| 6.2 | Test Setup | 72 |
| 6.3 | Calibration of the Solar Simulator | 72 |
| 6.4 | Result | 72 |

LIST OF TABLES

page

| | | |
|----------|--|----|
| TABLE 1: | Special Solder | 7 |
| 2: | Vacuum Hard-solder | 10 |
| 3: | Hard-soldering with Degussa Vacuum Hard-solder VH 570 | 11 |
| 4: | Hard-soldering with Degussa Vacuum Hard-solder VH 580 | 12 |
| 5: | Hard-soldering with Degussa Vacuum Hard-solder VH 640 | 12 |
| 6: | Welding Silver Foil (50) on Soldering Bar or Back Side of Cell. Cleaning the Contacts with Glass Hair Pencil (Electrode Pressure 500 p) | 17 |
| 7: | Welding Silver Foil (50) on Soldering Bar, Cleaning the Cell with J80 U | 18 |
| 8: | Welding 50 Silver Foil to Back Side of Cell; Cleaning the Cell with J80 U | 19 |
| 9: | Welding Silver Foil (50) to Soldering Bar with Strengthened Silver Layer; Cleaning with J80 U | 20 |
| 10: | Comparison Between Welding with Smooth and Projected Solder Connector | 21 |
| 11: | Dimensions of Various Types of Silver Mesh from the Exmet Corporation | 29 |
| 12: | Welds from Silver Mesh to Solar Cells | 30 |
| 13: | Comparison between Soldering and Welding Techniques of Connection | 32 |
| 14: | Thermal Vacuum Tests on Adhesives | 35 |
| 15: | Tensile and Shear Strength of Adhesives at Various Temperatures | 36 |

| | | |
|-----|---|----|
| 16: | Separation Tests on Partial Cover Glass Fastening (Spray Adhesive 77 from 3M) | 49 |
| 17: | Adhesive Strength of Thermodiffusion Connections | 53 |
| 18: | Cell Degradations by Cover Glasses | 54 |
| 19: | Losses of Weight of Connection Foil in the Thermal Vacuum | 58 |
| 20: | Climate Test | 67 |
| 21: | Measurement Values of the Thermal Balance Experiments | 75 |

| | LIST OF ILLUSTRATIONS | Page |
|-----------|--|---------|
| Figure 1: | Impulse heated tantalum electrode | 14 |
| 2: | Solder union of silver mesh Soldamoll 170 (silver grid is pressed flat below by the resistance electrode. Solder visible between the silver mesh grids.) | 14 |
| 3: | Cu/W Welding electrodes, welding on the front side of the cell | 22 |
| 4: | Cu/W Welding electrode, welding on the back side of the cell | 22 |
| 5: | Schematic of the Cu/W welding electrode | 24 |
| 6: | Silver mesh weld points (weld point on the silver mesh cross point) | 25 |
| 7: | Silver mesh weld points (weld point on the silver mesh cross point) | 25 |
| 8: | Welds on silver mesh grids | 26 |
| 9: | Weld on silver mesh grids | 26 |
| 10: | Separation apparatus (stress perpendicular to the solar cell) | 28 |
| 11: | Separation apparatus (stress parallel to the solar cell) | 28 |
| 12: | UV spectrum of the UV standard lamp (Philips model 126066, 250 W) | 39 |
| 13: | Transmission in the adhesive before and after UV irradiation Dow Corning XR-6-3489 | 41, 41a |
| 14: | Adhesive sample (type XR-6-3489) after UV irradiation | 43 |
| 15: | Coating the cover glass on the suction stub with adhesive | 44 |

| | | |
|-----|---|----|
| 16: | Evacuation and spring mounting for the solar cell | 44 |
| 17: | Applying a solar cell to the cover glass | 46 |
| 18 | Hardening the cover glass adhesive by IR irradiation | 46 |
| 19: | Cell after being torn from a cover glass fastened by thermodiffusion | 51 |
| 20: | Cover glass after being torn a cell fastened by thermodiffusion | 51 |
| 21: | Oven for connecting cover glass and cell by thermodiffusion | 52 |
| 22: | Quantum yield with and without a glued cover glass | 55 |
| 23: | Quantum yield with and without a loosely positioned cover glass | 56 |
| 24: | Module with welded solar cells (front side) | 63 |
| 25: | Welding module (back side) | 63 |
| 26: | Intermediary stages in the construction of a glass covered solar cell | 64 |
| 27: | Construction of a test module | 64 |
| 28: | Module with 2 solar cells and 2 second surface mirrors for the heat balance measurement | 65 |
| 29: | Test chamber for the heat balance measurement | 65 |
| 30: | Schematic of the test chamber | 70 |
| 31: | Equilibrium temperature of modules in the vacuum dependent on various insulators | 71 |

1. INTRODUCTION AND SUMMARY

1.1 Problem

The temperature appearing in the solar cell circuit of a solar probe can amount to between -60°C and $+200^{\circ}$ depending on the condition of the entire surface (spin stabilized, axis of spin perpendicular to the ecliptic). The light intensities thus acting on the solar cell vary between 0 and ca. 11 solar constants at distances from the sun of between 1.0 and 0.3 AE. The first part of this experimental study will report on the special characteristics of the solar cell, even at these extreme application demands. The object of the second part is to investigate the technological and physical problems which arise during the production of the solar cell panel. This deals with the following main elements:

- cell connection techniques (soldering, welding)
- cover glass bonding techniques (adhesion, thermodiffusion)
- application process (cementing the cell with isolating base foil and structure)
- module technique in connection with reflectors (second-surface mirrors).

The problems to be investigated relate to:

- optical and thermal behavior in the vacuum (measurement of

transparency, vaporizations, UV degradations,
heat gradients and other characteristics)

- mechanical behavior (static and dynamic stability with variable temperature)
- behavior during thermal shocks
- electrical behavior before and after production and test processes
- technical practicability

1.2 Course of the Study

The tasks summarized in the "Problem" section were completed under contract of the Siemens Company. Originally the studies were to begin in the middle of May and last 7½ months to the end of the year. At the beginning of September a verbal communication from the Society for Space Research informed us that the contract was to be granted to Siemens/Bölkow. On the strength of that, prepared studies were begun with the firm already in August. In November the SSR held out the prospect of an extension of the studies to 1-31-69; this was confirmed at the end of December.

Because of this shortening of the available time, some of the points in the originally planned program could not be intensively studied. In addition, there were several repeated program changes, which had changed the conceptions of a solar probe. Late delivery dates, especially for solder, foils and adhesives, caused further

delays. This effected in particular construction of the modules and their long-term tests as well as the measurements of the thermal balance of the module.

1.3 Summary of the Results

1.31 Cover Glass Assembly

In the temperature region from -60°C to 200°C as well as at solar intensities from 1 to 11 suns (140 mW/cm^2 to 1550 mW/cm^2) the use of the conventional cover glass assembly utilizing transparent adhesives is possible in principle. The behavior in the thermal vacuum as well as the separation tests at various temperatures support the use of the transparent adhesive XR - 6 - 3489 from Dow Corning. First irradiations with UV over a period of ca. 900 equivalent sun hours caused discolorations. A final pronouncement on UV degradations can only be made after further intensive studies have been completed.

Other connection techniques are possible. Partial gluings on the contact grid as well as connections by thermodiffusion between the cell grid and the cover glass grid were successfully achieved. The latter process is a significant step toward realizing solar cell modules without using organic materials. Further investigations, however, would be necessary in order to make the process practicable.

1.32 Cell connection

The most favorable connection technique proved to be welding

with silver mesh connectors (2AG5-6/0 Exmet) and Cu-W electrodes. The separation strengths were over 1000 p (reproducible). The applicability of this connection process may extend far beyond the temperature regions defined here (temperature behavior of silver). Thermal shock and vibration tests produced no changes. The electrical behavior before and after the welding remained unchanged. Contrary to expectations, the impulse welding process proved to be more practical than the soldering process applied earlier. It may also be more practical than the process for heatable solar cell circuits developed in the U.S.A. to secure the electrical cell connectors by means of thermodiffusion (Ref. 2)

1.33 Base Foil

The usual commercial Cu-Kapton connection foils are unstable in the vacuum at temperatures above 200° C (bubble formation due to volatilization of the adhesive). Some unions of Kapton and Cu foil with XR-6-3489 DC produced stable base foils after previous roughening of the Kapton foil by sand-blasting.

1.34 Complete Module

The results of tests on the module can be summarized as follows:

- Shock, climate and vibration tests caused no mechanical changes. The electrical degradation by tests as well as the production process lay within the limits of measurement accuracy.

- The load on the solar simulator extended to 19 solar constants (temperatures to 360° C, no reflectors).
- Measurements of the thermal balance on the module with reflectors (SSM) produced temperatures around 200° C at 11 solar constants with perpendicular radiation.

1.35 Module and Production Technique

The previous production technique and equipment were adapted to the new materials to be utilized and the new techniques. The new module technique showed itself to be more expedient than the earlier standard process aside from the extended temperature region for the module.

2. CELL CONNECTION

2.1 Investigated Connection Techniques

Main demands on the cell connections are:

- optimal electrical conductivity
- good mechanical adhesion
- temperature stability between -60° C and 200° C incl.
thermal shock stability
- minimal degradation of the solar cell
- simplest possible operation process
- simple exchangeability of damaged solar cells

For these demands soft-soldering, hard-soldering and welding connections are to be considered.

2.2 Soft-soldering

2.21 Selection of High-melting Soft-solder

The selection of the soft-solder was made on the basis of the highness of the melting point. One had to note, moreover, whether the alloy possessed an eutectic. Alloys with eutectics are usually indicated by smaller thermal shock and vibration stability. Alloys with saturated silver content were preferred since this prevented the vaporized silver layer of the solder bar on the solar cell from being attached during soldering.

Long delivery periods and late deliveries by the producer hindered the tests with soft-solder. Thus, only a small number of the soft-solder tests could be completed.

For normal use a low-melting solder was used: Soldamoll 170 (3% Ag, 37% Pb, 60% Sn, melting point 170° C). The required high temperature stability demanded higher melting solders. The special soft-solder of the Degussa Company was used.

The solder alloys formed are alloyed from materials at least 99.99% pure and are molten under vacuum. They are oxide-free and can thus also be utilized for complicated soldering without the use of fluxing agents. The solders 626, 627, 628 ought to be especially suitable for soldering which demands changes of temperature. With the exception of solders 612, 617, 626, 627 and 628,

TABLE 1
Special Soft-solder

| No. Nr. | Pb | Sn | In | Ag | Au | Other Sonst. | 1 Solidus °C | 2 Liquidus °C |
|------------|------|----|----|-----|----|-----------------|--------------------|---------------------|
| 605 | 95 | | | 5 | | | 304 | 370 |
| 606 | 92,5 | | 5 | 2,5 | | | 304 | 347 |
| 607 | 92 | 8 | | | | | 285 | 305 |
| 608 | 87 | 8 | | 5 | | | 294 | 397 |
| 609 | 83 | | 7 | 10 | | | 307 | 380 |
| 612 | 60 | 5 | | 32 | | 3 Bi | 290 | 577 |
| 618 | 9 | 15 | | | 76 | | 246 | 383 |
| 622 | | 95 | | | | 5 Cu | 227 | 375 |
| 629 | 90.8 | 8 | | 1,2 | | | 290 | 320 |

Legend: 1 - Solidification point; 2 - Melting point

be delivered in foil or stamped form, the delivery forms of the remaining alloys are wires, foils and stamped parts. Of the soft-solders in Table 1 only solders 608 and 609 could be investigated in conjunction with the present contract.

2.22 Soldering Process

Flux agents (Soldaflux A, rosin, or Castolin 154 C) were applied in alcoholic solution to the Ti - Ag contact layer by

means of brushes and were air dried before soldering or were applied as a paste over a template to the predetermined position. The cells were degreased prior to soldering with coloradol in an ultrasonic cleaner and were cleaned with 180 U from the Bandelin Company. 180 U dissolves sulfide and oxide layers on the soldering bars. Finally the cells were rinsed in distilled H_2O and washed after an alcohol bath. The cleansed cells were then placed in the soldering equipment and covered with a sheet of silver mesh (3 mm wide; Exmet Corp.; 2AG5-6/0) as the soldering connector with stamped soldering foil (1.5 x 0.05 mm, plated). The melting temperature of the solder was reached with a resistance heated tantalum electrode (cf. Fig. 1). A digital impulse welding apparatus from Hughes (Model Mc W550) was used. Adjustable parameters are impulse duration (1 ms - 10 s), the constant output potential (0 - 1 V) and the electrode contact pressure (0.5 - 2.4 Kp). The impulse was stimulated by foot pressure; triggering pressure and stopping pressure are identical. Every impulse forms a solder joint between the cell and soldering connector.

2.23 Results

The soldering parameters known for Soldamodel 170 were not suitable for the high-melting soft-solders and had to be changed. In order to reach sufficient, high-melting temperatures, soldering duration and output potential had to be greatly increased. This

shock-like increase of the temperature and the soldering point caused cell breakage in most cases before a complete flowing of the solder could be attained.

Separation tests showed that the joints thus formed were not genuine hot-solder joints but a bonding over the flux. A further temperature increase during soldering is not possible with this method of connection due to the sensitivity to breakage of the cells. Similar difficulties did not appear with standard Soldamoll 170 (melting point 180° C). Fig. 2 shows a silver mesh - Soldamoll joint.

2.3 Hard-soldering

2.31 Selection of Low-melting Hard-solders

The selection of the hard-solders was made on the basis of the highness of the melting temperature. Just as with soft-solder, hard-solders with eutectics can manifest a brittle behavior, which leads to difficulties during thermal shocks. High silver content of the hard-solder was desired to prevent a dissociation of the silver on the soldering strand. Solders containing cadmium were not considered on account of the high vapor pressure of cadmium. Long delivery periods of the alloys selected in the form of foils delayed the tests. The hard-solders which were used were vacuum hard-solders from the Degussa Company.

TABLE 2
Vacuum Hard-solders

| Lot 1 Nr. | Zusammensetzung 2 Gewichts-% | | | | Schmelz-3 bereich [°C] | Arbeits-4 temperatur [°C] | Anwendung für Werkstoffkombinationen 5 X = geeignet, — = bedingt geeignet | | | | | | | | | |
|--------------|---------------------------------|----|----|--------------------|------------------------------|---------------------------------|--|----|-------|-------|-------|-------|-------|-------|----------------|---------|
| | Ag | Au | Cu | Sonstige Other | | | Cu | Ni | Cu/Ni | Ni/Cu | Stahl | Fe/Co | Fe/Ni | Fe/Cr | Kovar Vacon | Mo W |
| VH 570 | 33 | 54 | — | 13 Ge | 530-550 | 570 | X | X | X | X | X | X | X | X | X | X |
| VH 580 | — | — | — | 88,3 Al 11,7 Si | 577 | 580 | — | — | — | — | — | — | — | — | X | X |
| VH 640 | 42 | — | 33 | 25 Sn | 635 | 640 | X | X | X | X | X | X | X | X | — | |

Legend: 1 - Solder No.; 2 - Content by weight - %; 3 - Melting region; 4 - Working temperature; 5 - Application for combinations of construction materials, x = suitable, - = unsuitable

The solder alloys formed are alloyed from materials at least 99.99% pure and are molten under vacuum. They are free of oxide and can thus also be used for complicated soldering without the utilization of flux agents. Forms delivered are wires, sheets, stamped parts and powder. Solder powers are delivered in grain sizes of 100 and 250 . HV 570 is only in the form of bands or stamped parts, VH 640 only in powder form.

2.32 Process

The solar cells were cleansed as in soft-soldering and placed in a mounting, covered by cleansed silver mesh (Exmet Corporation 2 AG5-6/0) with hard-solder foil (50μ thick, 1 mm^2), or with solder VH640, covered with dry soldering powder, and hard-soldered with the Hughes impulse welder. Molybdenum electrodes

(Hughes ESQ-2545-00) with a 0.1 mm gap were used as welding electrodes. The electrode pressure was varied between 1 kp and 1.5 kp the potential between 1.35 V and 1.99 V, and the impulse duration between 0.45 s and 9.5 s. The hard-soldering was done partially with and partially without flux. The separation strength was measured perpendicular to the surface of the solar cells (cf. Fig. 10).

2.33 Results

The results are summarized in the following tables:

TABLE 3

Hard-soldering with Degussa Vacuum Hard-Solder (33% Ag; 54% Au; 13% Ge; foil of 50 μ thickness)

| Flux Flußm. | | Welding Schweiß- spannung potential V | Welding Schweiß- dauer. duration ms | Electrode Elektroden- druck pressure kp | Separation Abreiß- kraft +) strength +) p |
|----------------|-----|---|---|---|---|
| nein | no | 1,95 | 950 | 1,0 | 0 |
| ja | yes | 1,95 | 950 | 1,5 | 800 |
| ja | yes | 1,95 | 950 | 1,5 | 0 |
| ja | yes | 1,95 | 950 | 1,5 | 500 |
| ja | yes | 1,75 | 950 | 1,5 | 225 |
| ja | yes | 1,75 | 950 | 1,5 | 0 |

+) at 8 mm solder width with 4 impulses

TABLE 4

Hard soldering with Degussa Vacuum Hard-solder VH 580
(88.3% Al; 11.7% Si; foil of 50 μ thickness)

| Flux Flußm. | Welding Schweiß- spannung potential V | Welding Schweiß- dauer duration ms | Electrode Elektroden- druck pressure kp | Separation Abreiß- kraft +) strength +) p |
|----------------|---|--|---|---|
| ja yes | 1,35 | 450 | 1,0 | 0 |
| ja yes | 1,55 | 450 | 1,0 | 0 |
| ja yes | 1,55 | 650 | 1,0 | 0 |
| ja yes | 1,75 | 650 | 1,0 | 0 |
| nein no | 1,99 | 750 | 1,0 | 0 |
| nein no | 1,99 | 750 | 1,4 | 0 |
| nein no | 1,99 | 750 | 1,4 | 0 |
| nein no | 1,99 | 950 | 1,4 | 0 |
| nein no | 1,5 | 9500 | 1,4 | 0 |
| nein no | 1,5 | 550 | 1,4 | 400 |

+) at 8 mm solder width with 4 impulses

TABLE 5

Hard-soldering with Degussa Vacuum Hard-solder VH 640
(42% Ag; 33% Cu; 25% Sn; powder grain size < 100 μ)

| Flux Flußm. | Welding Schweiß- spannung potential V | Welding Schweiß- dauer duration ms | Electrode Elektroden- druck pressure kp | Separation Abreiß- kraft +) strength +) p |
|----------------|---|--|---|---|
| ja yes | 1,75 | 500 | 1 | 0 |
| ja yes | 1,75 | 900 | 1 | 0 |
| ja yes | 1,75 | 900 | 1 | 0 |
| ja yes | 1,75 | 900 | 1,5 | 500 |

+) at 8 mm solder width with 4 impulses

As can be seen from Tables 3-5, the necessarily high temperatures during hard-soldering led to cell breakage in most cases (separation strength 0), so that no reproducible connections could be fabricated.

In part adhesion took place, but this was caused by flux adhesion. Because of the shortness of available time, very few tests could be completed. Using smaller quantities of hard-solder (thinner solder foil) could have led to better results. The good results from the welding technique (cf. Ch. 2.4) made further hard-solder experiments unnecessary.

2.4 Welding

2.41 General Comments

Silver foil and silver mesh proceeded as in 2.2. The cleaning of the silver contact layer on the cell with an eraser pencil or glass hair proved to be too coarse since the layer strength of the silver is only a few μ thick.

The welds were accomplished with the Hughes impulse welder. Since at first the proper kind of silver mesh was not available, work was begun with a 50 μ silver foil. The welding electrodes used here consisted of molybdenum (Hughes ESQ - 1525 -00). Shape and material were later changed with mesh welds. Our experiences are summarized in the following.

2.42 Welding Smooth Silver Foil

The first tests already showed that the welding method is

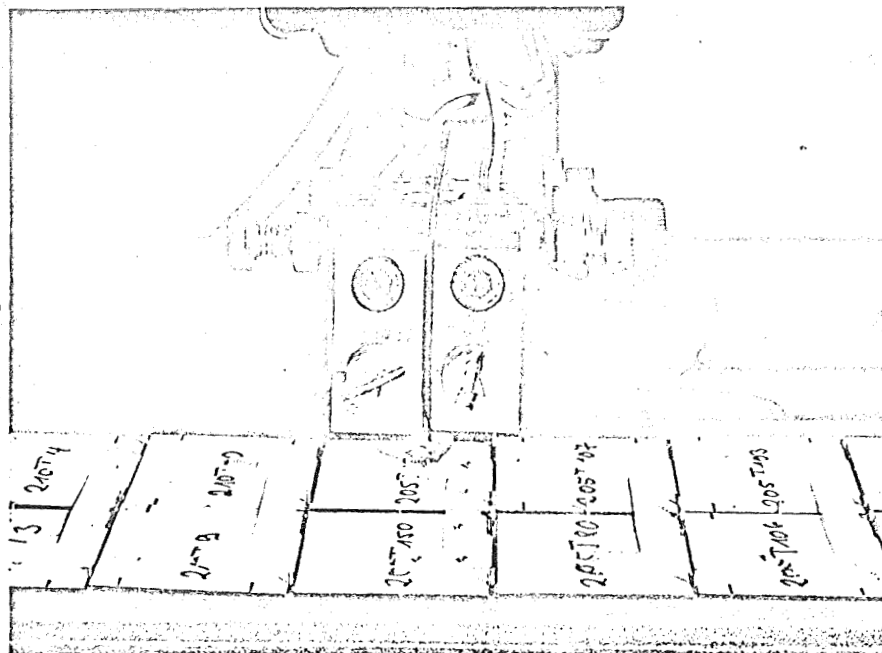


Fig. 1 Impulse heated tantalum electrode



Fig. 2 Solder union of silver mesh Soldamoll 170 (silver grid is pressed flat below by the resistance electrode. Solder visible between the silver mesh grids.)

very suitable for the connection of solar cells (Table 6). A 50 μ strong Ag foil was directly welded. Table 6 shows the forces that are necessary to tear a 1 mm wide Ag foil strip perpendicularly from the solar cell. Welding potential and time were varied also. In part cells stored for a longer time, whose contact layers were yellowed by oxidation and sulfide formation, were used. Experiments with molybdenum electrodes with increased contact surface (Hughes ESQ 2545-00) brought about only minor improvements.

With smooth silver foil the transition resistance to the silver layer of the solar cell is generally very diversified, so that the adhesion after welding was very irregular. Raising the welding potential or lengthening the welding time often caused the silver foil to be fused outside the welding point, so that the foil itself tore near the weld during separation tests. Normally the separation occurred in the weld, however.

Tables 7 and 8 show further results of welding samples. With these tests the cell was previously cleaned with J80U. A small increase in the separation strength could be attained.

Increasing the silver layer on the solar cells three, four and fivefold produced no better results (see Table 9). A significant increase in the welding time, however, brought good results. The experiment with surrounding the electrodes with argon as a protective gas did not lead to better results.

2.43 Welding Silver Foil by the Projection Welding Method

With this method a double depression (0.7 mm proximity, depth 60μ , rim ϕ ca. 0.1 mm, 90° cone point) is impressed in the silver sheet, so that the weld points are determined after applying the flat electrodes. Welding with the projection welding method produced a more regular adhesion. This is based on the apparently smaller transition resistivity between the foil and the cell. Both methods of welding (projection, smooth) were tried on a cell type (Siemens type V).

2.44 Welding Silver Mesh

Tests with the projection welding method allow one to expect a good connection when welding silver mesh. The first experiments in which silver mesh was welded with silver mesh confirm this suspicion. Under strain the silver mesh tear before the weld point for these welds.

The optimal welding of silver mesh is highly dependent on the structure, flexibility and thickness of the mesh. Therefore, extensive pre-tests were undertaken on various types of mesh (Exmet Corporation 2 AG5-6/0; 5 AG5-6/0, 5 AG5-5/0; 2 AG10-2/OE; Table 11). After the selection of suitable silver mesh types, various solar cells were welded with molybdenum electrodes (Hughes - 1525 - 00). The separation strengths with the stress perpendicular to the cell lay between 450 and 600 p. (Table 12).

TABLE 6

Welding Silver Foil (50 μ) to Soldering Bars or the Cell Backside. Cleaning the Contacts with a Glass Hair Brush (electrode pressure 500 p)

| Welding Schweiß- spannung (V) | Welding Schweiß- dauer (ms) | Abreiß- kraft (p) pro Schweiß- punkt | Separation force per weld point | Welding Schweiß- spannung (V) | Welding Schweiß- dauer (ms) | Abreiß- kraft (p) pro Schweiß- punkt | Separation force per weld point |
|--|--------------------------------------|---|---------------------------------------|--|--------------------------------------|---|---------------------------------------|
| 0,8 | 200 | 100 | Zelle 266M66 | 0,8 | 35 | 40 | Zelle 269T40 |
| 0,8 | 150 | 130 | vergilbt; | 0,8 | 30 | 40 | vergilbt; |
| 0,8 | 100 | 150 | Zellengrid | 0,8 | 40 | 50 | Zellengrid |
| 0,8 | 80 | 160 | | 0,8 | 45 | 70 | |
| 0,8 | 250 | 150 | Zelle 266M66 | 0,8 | 45 | 60 | |
| 0,8 | 200 | 160 | vergilbt; | 0,8 | 45 | 70 | |
| 0,8 | 150 | 170 | | 0,8 | 40 | 80 | Zelle 269T40 |
| 0,8 | 100 | 165 | Zellenunterseite | 0,8 | 35 | - | vergilbt; |
| 0,8 | 80 | 100 | | 0,8 | 50 | 70 | |
| 0,8 | 60 | 160 | | 0,8 | 55 | 60 | Zellenunterseite |
| 0,8 | 50 | 140 | | 0,8 | 55 | 50 | |
| 0,8 | 40 | 200 | | 0,8 | 60 | 60 | |
| 0,8 | 100 | 170 | Zelle 266M42 | 0,8 | 65 | 50 | |
| 0,8 | 80 | 140 | vergilbt; | 0,8 | 70 | 90 | |
| 0,8 | 60 | 190 | Zellengrid | 0,8 | 60 | - | Zelle 282T120 |
| 0,8 | 50 | 110 | | 0,8 | 70 | 60 | |
| 0,8 | 40 | 110 | | 0,8 | 80 | - | Zellengrid |
| 0,8 | 200 | 135 | Zelle 266M42 | 0,8 | 80 | 110 | |
| 0,8 | 150 | 120 | vergilbt; | 0,8 | 90 | 180 | |
| 0,8 | 150 | 130 | Zellenunter- | 0,8 | 100 | 130 | |
| 0,8 | 80 | 160 | seite | 0,8 | 110 | 70 | |
| 0,7 | 80 | 90 | | 0,8 | 60 | 40 | Zelle 282T120 |
| 0,9 | 80 | 130 | | 0,8 | 70 | 60 | |
| 0,8 | 35 | 20 | | 0,8 | 80 | 50 | Zellenunterseite |
| 0,8 | 30 | 10 | Zelle 266M61 | 0,8 | 90 | 60 | |
| 0,8 | 40 | 30 | vergilbt; | 0,8 | 100 | 60 | |
| 0,8 | 45 | 10 | Zellengrid | 0,8 | 110 | 90 | |
| 0,8 | 45 | 50 | | 0,8 | 120 | 100 | |
| 0,8 | 45 | 40 | | 0,8 | 130 | 90 | |
| 0,8 | 40 | - | Zelle 266M61 | 0,8 | 140 | 90 | |
| 0,8 | 35 | 50 | vergilbt; | 0,8 | 150 | 80 | |
| 0,8 | 50 | 90 | Zellengrid | | | | |
| 0,8 | 55 | 40 | | | | | |
| 0,8 | 55 | 70 | | | | | |
| 0,8 | 60 | 60 | | | | | |
| 0,8 | 65 | 40 | | | | | |
| 0,8 | 70 | 60 | | | | | |

key: Zelle = cell
vergilbt = yellowed
Zellengrid = cell grid
Zellenunterseite =
cell underside

TABLE 7

Welding Silver Foil (50 μ) to Solder Bars, Cell Cleaned
with J890 U

| Cell Zellen Nr. No. | Welding Schweiß- spannung potential V | Welding Schweiß- zeit time ms | Electrode Elektroden- druck pressure p | Separation Abreiß- kraft per weld pro Schweiß- punkt point p |
|------------------------------|---|---|--|--|
| 292T88 | 1 | 30 | 500 | 50 |
| | 1 | 30 | 500 | 0 |
| | 0,9 | 30 | 500 | 80 |
| | 0,8 | 30 | 500 | 0 |
| | 0,8 | 30 | 500 | 150 |
| | 0,7 | 30 | 500 | 0 |
| 291T75 | 0,7 | 35 | 500 | 0 |
| | 0,8 | 40 | 500 | 200 |
| | 0,9 | 40 | 500 | 40 |
| | 0,9 | 50 | 500 | 80 |
| | 0,9 | 20 | 500 | 50 |
| | 0,8 | 30 | 500 | 0 |
| 291T14 | 0,8 | 30 | 500 | 0 |
| | 0,8 | 20 | 500 | 0 |
| | 0,7 | 40 | 500 | 0 |
| | 0,7 | 40 | 500 | 0 |
| | 0,7 | 50 | 500 | 0 |
| | 0,7 | 60 | 500 | 0 |
| 291T18 | 0,8 | 60 | 500 | 0 |
| | 0,7 | 60 | 500 | 0 |
| | 0,8 | 30 | 500 | 0 |
| | 0,9 | 20 | 500 | 0 |
| | 0,9 | 20 | 500 | 0 |
| | 0,8 | 30 | 500 | 0 |
| 282T27 | 0,8 | 150 | 500 | 120 |
| | 0,8 | 70 | 500 | 230 |
| | 0,8 | 70 | 500 | 20 |
| | 0,8 | 60 | 500 | 0 |
| | 0,8 | 60 | 500 | 0 |

TABLE 8

Welding 50 μ Silver Foil to the Underside of the Cell,
Cell Cleaned with J80 U

| Cell Zellen Nr. | Welding Schweiß- spannung V | Welding Schweiß- zeit ms | Electrode Elektroden- druck p | Separation Abreiß- kraft pro Schweiß- punkt p |
|-----------------------|--------------------------------------|-----------------------------------|--|--|
| 282T146 | 1,0 | 30 | 500 | 170 |
| | 1,0 | 30 | 500 | 0 |
| | 1,0 | 30 | 500 | 120 |
| | 1,0 | 30 | 500 | 200 |
| | 1,0 | 30 | 500 | 0 |
| | 0,9 | 30 | 500 | 0 |
| | 0,9 | 30 | 500 | 60 |
| | 0,9 | 30 | 500 | 60 |
| | 0,9 | 30 | 500 | 180 |
| | 0,8 | 30 | 500 | 30 |
| | 0,8 | 30 | 500 | 30 |
| 282T147 | 1,0 | 30 | | 150 |
| | 1,0 | 30 | | 60 |
| | 1,0 | 30 | | 170 |
| | 1,0 | 30 | 500 | 210 |
| | 1,0 | 30 | 500 | 0 |
| | 1,0 | 30 | 500 | 220 |
| | 1,0 | 30 | 700 | 280 |
| | 1,0 | 30 | 800 | gebr. |
| | 1,0 | 30 | 350 | 190 |
| | 1,0 | 30 | 350 | 170 |
| | 1,0 | 30 | 350 | 260 |
| | 1,0 | 30 | 350 | 210 |
| | 1,0 | 30 | 350 | 270 |
| | 1,0 | 30 | 350 | 350 |
| 282T151 | 1,1 | 30 | 500 | 180 |
| | 1,2 | 30 | 500 | 120 |
| | 1,2 | 30 | 500 | 80 |
| | 1,2 | 30 | 500 | 240 |
| | 0,9 | 30 | 500 | 230 |
| | 0,9 | 30 | 500 | 230 |
| | 0,9 | 30 | 500 | 180 |
| | 0,9 | 30 | 500 | 170 |
| | 0,8 | 30 | 500 | 170 |
| | 0,8 | 30 | 500 | 80 |
| 282T174 | 0,9 | 30 | 500 | 190 |
| | 0,8 | 30 | 500 | 150 |
| | 0,8 | 30 | 500 | 120 |
| | 0,8 | 30 | 500 | 150 |
| | 0,7 | 30 | 500 | 0 |
| | 0,7 | 30 | 500 | 0 |
| | 1,0 | 30 | 500 | 200 |
| | 1,0 | 30 | 500 | 110 |
| | 0,9 | 30 | 500 | 150 |
| | | | | |

TABLE 9

Welding Silver Foil (50 μ) to Solder Bars with Strengthened Silver Layer, Cleaning with J80 U.

| Cell No. | Welding potential V | Welding time ms | Electrode pressure p | Separation force per weld point p |
|--------------|------------------------|--------------------|-------------------------|--------------------------------------|
| 293T116 | 1 | 30 | 500 | 0 |
| | 0,9 | 30 | 500 | 0 |
| Grid with | 0,8 | 30 | 500 | 5 |
| 4-fold quan- | 0,8 | 30 | 500 | 250 |
| tity of Ag | 0,8 | 30 | 500 | 100 |
| 293T106 | 0,7 | 30 | 500 | 0 |
| | 0,8 | 30 | 500 | 60 |
| Grid with | 0,85 | 30 | 500 | 20 |
| 3-fold quan- | 0,83 | 30 | 500 | 50 |
| tity of Ag | 0,63 | 330 | 500 | 600 |
| | 0,58 | 400 | 500 | 400 |
| 282T174 | 0,58 | 400 | 500 | 200 |
| | 0,58 | 400 | 500 | 270 |
| | 0,58 | 400 | 500 | 260 |
| 293T106 | 0,63 | 400 | 500 | 400 |
| Grid with | 0,63 | 400 | 500 | 250 |
| 3-fold quan- | 0,63 | 400 | 500 | 425 |
| tity of Ag | 0,63 | 400 | 500 | 500 |
| | 0,63 | 400 | 500 | 350 |
| Grid with | 0,63 | 400 | 500 | 500 |
| 4-fold quan- | 0,63 | 400 | 500 | 350 |
| tity of Ag | 0,63 | 400 | 500 | 550 |
| | 0,63 | 400 | 500 | 650 |

TABLE 10

Comparison Between Welding with Smooth and Projection
Solder Connector, foil thickness: 50 μ cell type 282T 114

| Welding Schweiß- potential spannung V | Welding Schweiß- time zeit msec | Electrode Elektroden- pressure druck p | Separation Abreiß- force kraft p +) |
|--|---|--|---|
| Solder connector Lötverbinder glatts smooth | | | |
| 1.0 | 30 | 600 | 0 |
| 1.1 | 30 | 600 | 0 |
| 1.2 | 30 | 600 | 0 |
| 0.9 | 30 | 600 | 0 |
| 0.8 | 30 | 600 | 0 |
| Solder connector Lötverbinder gebuckelt projection | | | |
| 0.92 | 80 | 600 | 180 |
| 1.02 | 80 | 600 | 250 |
| 0.82 | 80 | 600 | 280 |
| 0.72 | 80 | 600 | 380 |

+) per weld point

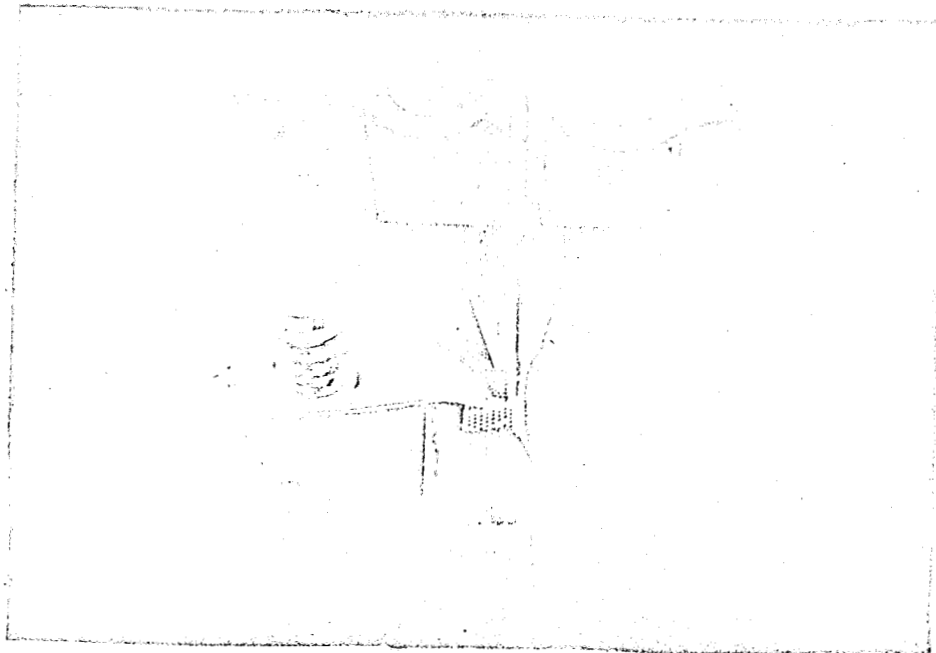


Fig. 3 Cu/W Welding electrodes, welding on the front side of the cell

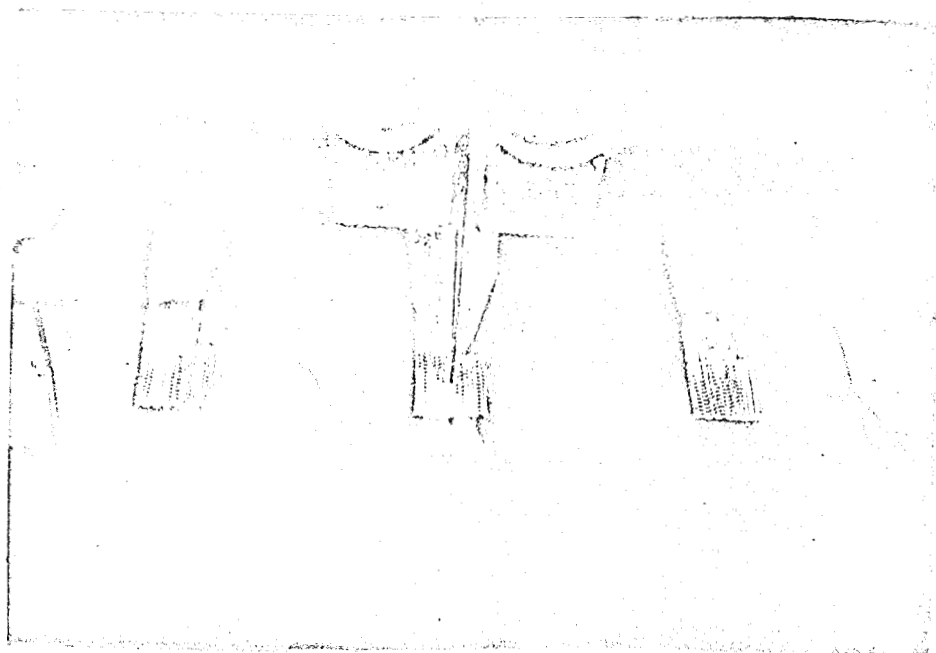


Fig. 4 Cu/W Welding electrode, welding on the back side of the cell

However, a knife-like tantalum electrode produced separation strengths between 800 and 1200 p. Because of the short working life of the Ta electrode due to oxidation, another electrode material had to be sought. A Cu electrode combined with a Mo electrode was used. Simultaneously the even electrode pressure of 500 p was changed so that one electrode (Cu) was applied with a 250 p force and the other with 600 p. Welds with this electrode combination produced separation strengths of 1200 p (Table 12). The working life of the molybdenum electrode was also too short, and the electrode was replaced by a tungsten electrode. With this electrode combination separation forces between 300 p and over 2.4 kp were obtained.

After setting the welding parameters at 0.6V welding potential and 420 ms welding duration at an electrode pressure of 250 p and 600 p, separation forces of ≥ 1000 p resulted (Table 12). The separation (perpendicular to the cell surface) occurred not in the weld point but in the silver mesh itself.

Figures 6 and 7 show microscopic photos of silver mesh weld points as they are formed at the W electrode, which presses down harder on the grid strand. Figures 8 and 9 show welds on the grids instead of on the mesh cross points. (The welding zones are recognizable as lighter patches). The location of the welding zone, whether mesh cross point or mesh grid, is dependent on the positioning or the cut of the mesh in the cutting equipment but does not effect the quality of the weld.

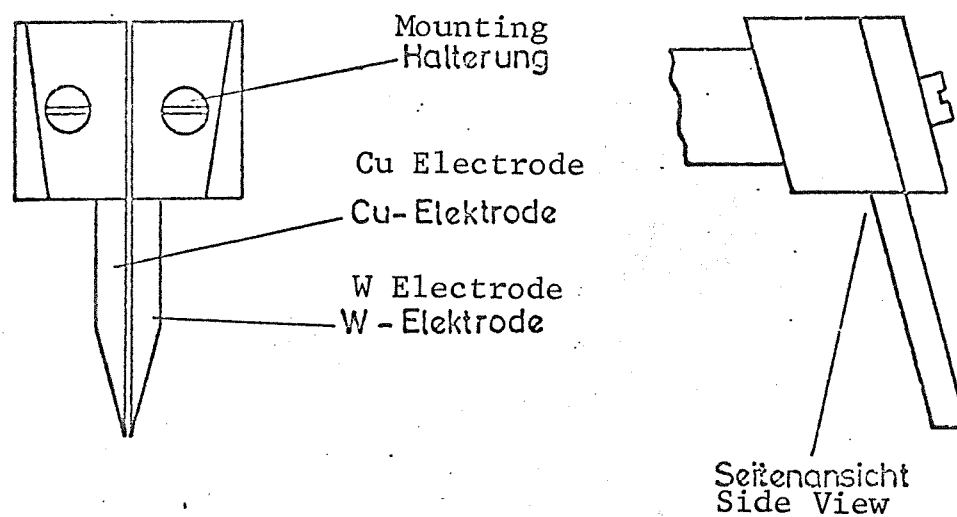


Fig. 5 Schematic of the Cu/W welding electrode

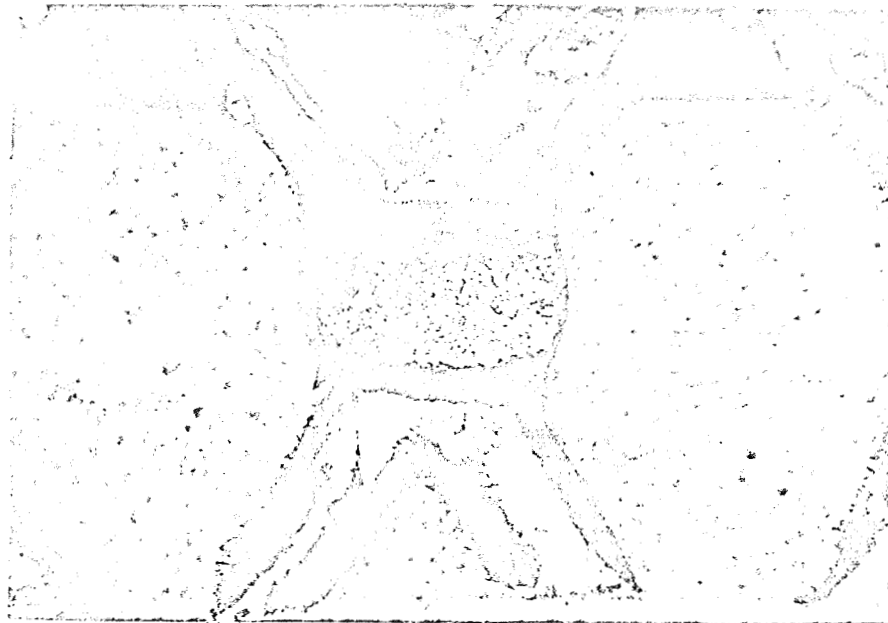


Fig. 6 Silver mesh weld points (weld point on the silver mesh cross point)

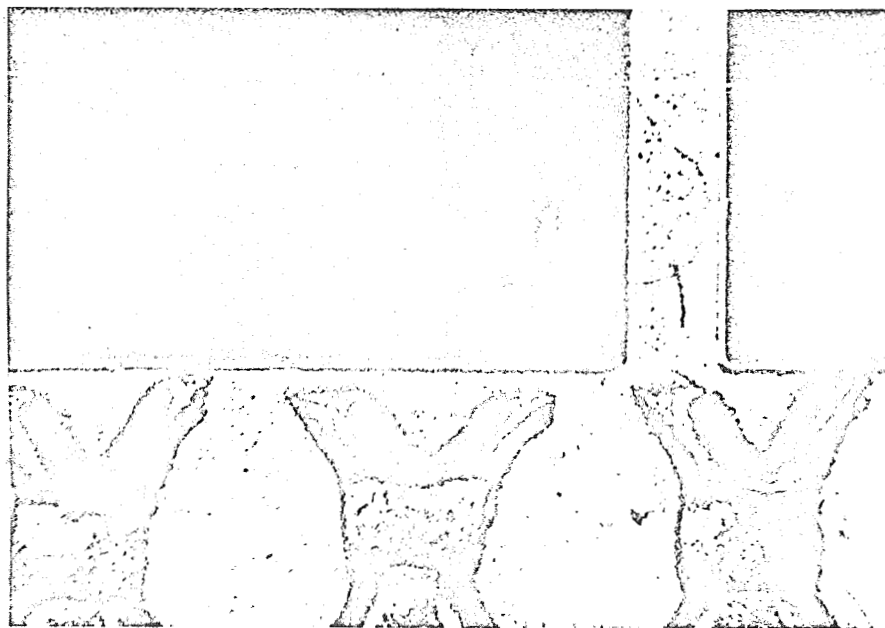


Fig. 7 Silver mesh weld points (weld point on the silver mesh cross point)

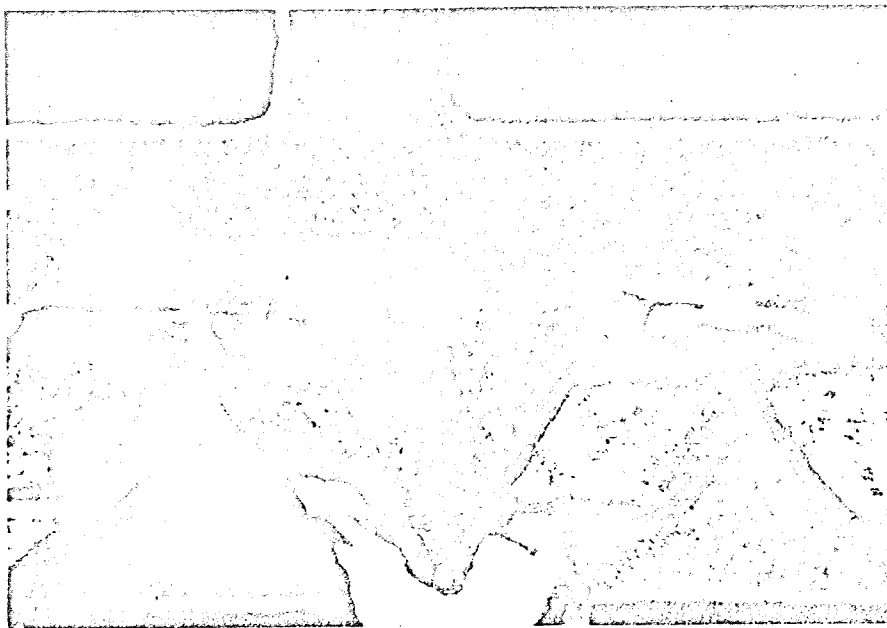


Fig. 8 Welds on silver mesh grids

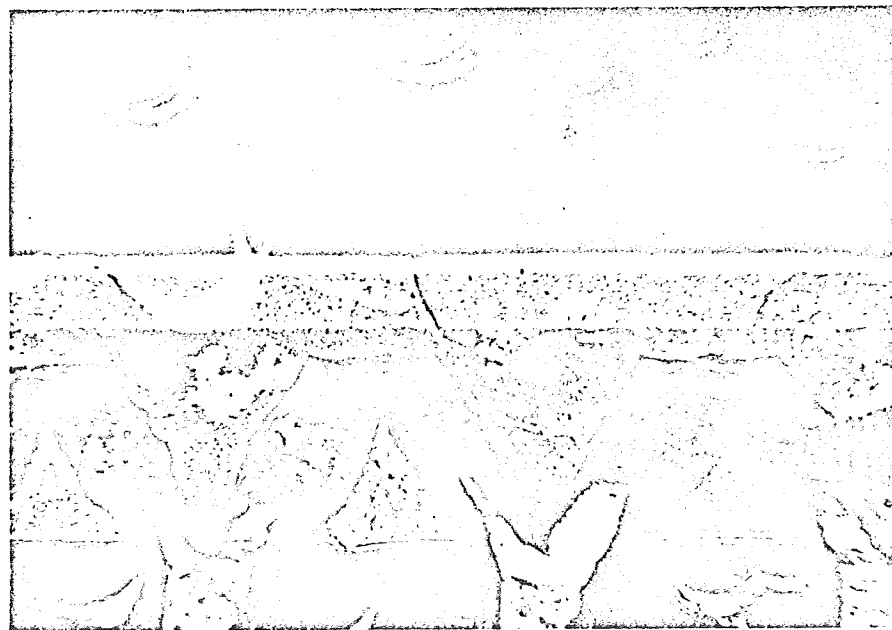


Fig. 9 Weld on silver mesh grids

2.45 Conclusions

Because of the high separation strength when impulse welding connections to solar cells, the welding method with silver mesh is eminently suitable for the production of solar cell modules. No loss of cells due to breakage or flaws during welding or other mechanical damage could ever be determined. After setting the welding parameters on the basis of the separation tests (0.6 V, 420 s, 250/600 p, Cu/W electrodes), they were tested by electrical measurements for degradation before and after welding. (Measurement of the short-circuit current with brief illumination to prevent uncontrolled increases in temperature.) The measurements showed no degradation outside the measurement accuracy of the equipment used (<2%).

The following tests were completed on individual welding connections:

Shock test: -196°C (fl. nitrogen) - $+ 80^{\circ}$ (H_2O) ca. 20 times

Separation test: (stress vertical) separation strength

100 p, mesh tore (fig. 10)

Separation test: (shearing stress) separation strength

2500 p, mesh tore (fig. 11).

The separation in the shear direction (parallel to the surface of the solar cells) is even higher than that perpendicular to the solar cell surface since with the latter the stress usually leads

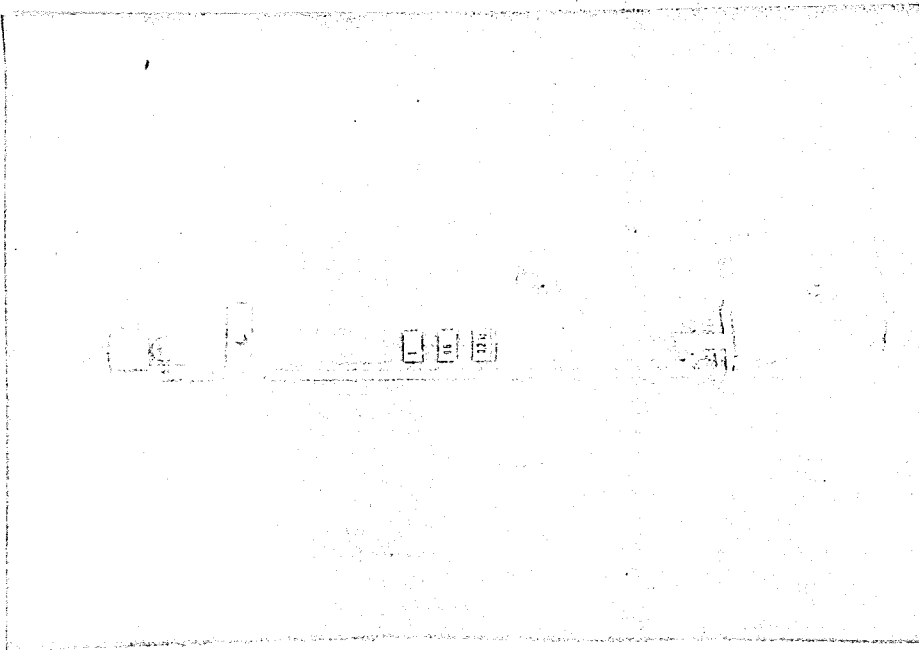


Fig. 10 Separation apparatus (stress perpendicular to the solar cell)

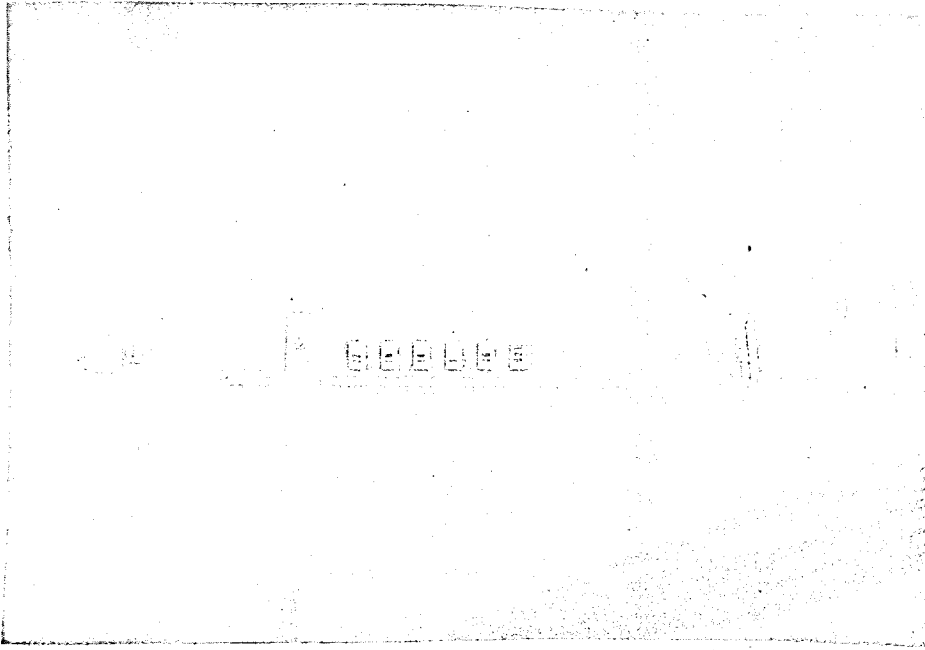




Fig. 11 Separation apparatus (stress parallel to the solar cell)

TABLE 11

Dimensions of Various Types of Silver Mesh from the
Exmet Corporation

| MESH DESIGNATION (Size) | MESH DIMENSIONS From center-to-center of joints | | Number openings per sq. in. approx. | THICKNESS OF ORIGINAL MATERIAL | | STRAND WIDTH | | MAX. SHEET WIDTH |
|-------------------------------|---|-------------|--|--|-------|--|-------|------------------------|
| | min. | max. | | MIN.  | MAX. | MIN.  | MAX. | |
| 1 | .405" | .20" .23" | 25 | .003" | .025" | .007" | .055" | 12" |
| 1/0 | .280" | .10" .125" | 65 | .003" | .025" | .007" | .055" | 12" |
| 2/0 | .187" | .077" .091" | 120 | .002" | .020" | .007" | .035" | 12" |
| 2/0E | .187" | .048" .071" | 170 | .002" | .015" | .007" | .035" | 12" |
| 3/0 | .125" | .050" .065" | 300 | .002" | .015" | .003" | .020" | 12" |
| FS | .100" | .075" .085" | 250 | .005" | .020" | .007" | .025" | 12" |
| 4/0 | .077" | .038" .046" | 625 | .002" | .010" | .003" | .020" | 10" |
| 5/0 | .050" | .026" .030" | 1400 | .002" | .010" | .002" | .011" | 6" |
| 6/0 | .031" | .021" .024" | 2600 | .002" | .007" | .002" | .003" | 5" |

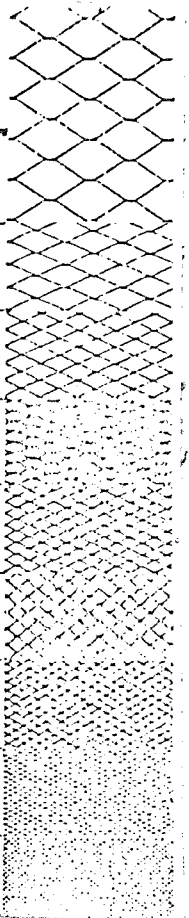


TABLE 12

Welding Silver Mesh to Solar Cells

| Cell No. | Welding potential V | Welding duration ms | Electrode pressure p | Separation strength at 8 mm weld width 4 impulses p |
|-----------|------------------------|------------------------|-------------------------|--|
| 293T116 | 0,50 | 330 | 350 | 600 Mo- |
| Grid | 0,50 | 330 | 500 | 450 Electrodes |
| 293T106 | 0,50 | 330 | | 600 |
| Grid | | | | |
| 293T109 | 0,63 | 400 | 600 | 800 Ta- |
| Grid | | | | Electrodes |
| 282T147 | 0,63 | 400 | 600 | 800 " |
| Grid | | | | |
| 293T114 | 0,63 | 400 | 600 | 1200 " |
| Grid | | | | |
| 269T23 | 0,53 | 400 | 250; 600 | 1200 Cu-Mo- |
| Grid | 0,63 | 400 | 250; 600 | 1200 Electrodes |
| 282T99 | 0,58 | 400 | 250; 600 | 300 |
| Grid | 0,60 | 400 | 250; 600 | 600 |
| | 0,62 | 420 | 250; 600 | 800 |
| | 0,62 | 420 | 250; 600 | 900 |
| | 0,63 | 420 | 250; 600 | 1000 |
| 293T117 | 0,60 | 420 | 250; 600 | 1000 Cu, W- |
| Grid | | | | Electrodes |
| 293T114 | 0,60 | 420 | 250; 600 | 600 |
| back side | 0,58 | 440 | 250; 600 | 800 |
| | 0,56 | 460 | 250; 600 | 950 |
| | 0,55 | 500 | 250; 600 | 850 |
| 270Z32 | 0,54 | 620 | 250; 600 | 1000 |
| Grid | | | | |
| 270Z33 | 0,60 | 400 | 250; 600q | 1000 |
| Grid | | | | |
| 299T55 | 0,60 | 420 | 250; 600 | 2400 |
| Grid | | | | |
| 282T42 | 0,60 | 420 | 250; 600 | 1250 |
| back side | | | | |
| 82T114 | 0,60 | 420 | 250; 600 | 1600 |
| Grid | | | | |

to separation of the individual weld points one after another. No difference could be determined further between weld stability on the solder strand or on the reverse side of the cell. With the tests cited there were no changes at all, either visual or electrical (short-circuit current). With respect to vibration stability see Ch. 5.

2.5 Comparison of the Processes

In Table 13 the most important criteria for judging the welding and soldering connection techniques were given.

The first preliminary investigations had already shown that the welding connections could be produced easier, more quickly, and with better control than the high-temperature solder connections. Thus, more and more emphasis was placed on the welding technique. By eliminating time-robbing work processes like the cleaning operation and preliminary treatment for the soldering technique, as well as by having a small rate of failure, the welding technique could be considered much more practical. It is equally suitable for practically every form of solar panel and for all applications (especially for lightweight circuits). The section "Module Construction" will deal with new possibilities for module construction (production methods other than those now common).

The good adhesion of the cells Ti - Ag layer is essential for the reliability of all techniques of connection. The cells delivered (according to Siemens specifications type IV and later type V) fulfilled these demands.

TABLE 13 Comparison between Soldering and Welding Techniques

| Criteria | Welding | Hard or soft soldering with high-melting solders |
|---|---|--|
| Cleaning process before connection after connection | Not definitely desirable Not desirable | Desirable Desirable |
| Degradation by connection technique | None | Frequent cell breakage Danger of hair-line cracks |
| Influence of the connection technique on other module components | None | Flux can attach the adhesive |
| Coefficient of thermal expansion between connector and contact material | Same | Different |
| Control of connection parameters | Easy | Difficult (flux-solder dosage) |
| Disintegration temperature | Ag melting point (960°C) | 300° to 635° C |
| Behavior with respect to dampness | Not sensitive | Not investigated |
| Climate, shock and vibration tests | No changes | Not investigated |
| Interchangeability during production of module | Easy | Difficult |
| Separation strength | >1000 p reproducible | Not reproducible (Neither hard nor soft-solder produced a reducible connection) |
| Costs | Optimal | High (high rate of failure; long course of manufacture) |

3. COVER GLASS ASSEMBLY

3.1 Possibilities for Cover Glass Assembly

Various processes are available for the cover glass assembly of solar cells.

- complete bonding of surface with transparent (optical) adhesives
- bonding at points with non-optical adhesives
- mechanical mounting for the cover glasses
- connection by thermodiffusion (between the cell grid and a grid on the cover glasses equivalent to a cover

Mechanical mounting of the cover glasses on solar cells was rejected since it would incur significant disadvantages like high weight and large volume. In the following, bondings with optical and non-optical adhesives and bonding by thermodiffusion were investigated.

The use of optical adhesives caused various problems:

- changing the degree of transmission by UV radiation
- thermal vacuum behavior
- adhesion at various temperatures.

Non-optical adhesives which connected the cover glass and cells at points or bands also gave the same problems, in part:

- thermal vacuum behavior
- adhesion at an increased temperature
- adhesion at very small adhesive surfaces

- lessening the degree of effect of the solar cells as a result of diminishing the active surface by adhesive points
- lessing the degree of effect of the solar cells as a result of a non-optimal index of refraction transition (crack between cell and cover glass).

3.2 Optical Adhesives

The adhesives studied were from the Wacker, Dow Corning and General Electric companies. Similarly, non-optical adhesives were investigated for the panel assembly.

3.21 Thermal Vacuum Behavior

To study the thermal vacuum behavior of adhesives two small aluminum blocks were glued together with various adhesives and set out in a vacuum between 10^{-5} and 10^{-6} torrs with temperatures of 200° C. The duration of the test was from 24 to 67 hours. The samples were then studied for weight loss, shear and tensile strength. The results are shown in Table 14. It was evident that the optical adhesive XR-6-3489 (Dow Corning) showed the best values. This underwent, in addition, a long-term test of 410 hours in the thermal vacuum (240° C, 10^{-6} torrs. Loss of weight amounted to 4.6%. No visual changes could be recognized.

3.22 Adhesion of Optical Adhesives at Various Temperatures

The adhesives XR-6-3489 (Dow Corning) and Sil gel 2000 (Wacker) were tested.

TABLE 14 Thermal Vacuum Tests of Adhesives (See key p. 36)

| Nr. | Kleber | Temperat. | Dauer des Versuchs | Druck (Torr) | Gewichtsverlust | Zugversuch Kp/cm^2 | Scherversuch Kp/cm^2 | Bemerkungen |
|-----|--------------------------------|-----------|--------------------|-------------------|-----------------|---------------------------------|-----------------------------------|---|
| 1 | Talkum und Waserger 10 (1:1,4) | 200°C | 67 Std. hours | $6 \cdot 10^{-6}$ | 6,4 % | 1,3 | beim Versuchsaufbau zerbrochen 11 | 1/2 Tag ausgehärtet; Bruch im Kleber 12 |
| 2 | Talkum und Waserger 10 (1:1,3) | 300°C | 24 Std. | $6 \cdot 10^{-6}$ | +0,12 % | 0,8 | 3,55 | 12 Std. ausgehärtet; Bruch im Kleber 13 |
| 3 | Talkum und Waserger 10 (1:1,3) | 400°C | 24 Std. | 10^{-5} | +0,05 % | 1,33 | beim Versuchsaufbau zerbrochen 11 | 24 Std. ausgehärtet; beim Zugvers. Bruch im Kleber; beim Scherversuch glasartige Schicht, an der die Probe zerbrach 14 |
| 4 | RTV 3145 | 200°C | 24 Std. | $4 \cdot 10^{-6}$ | 0,59 % | 3,4 | 3,5 | geprimert; 24 Std. ausgehärtet; Bruch im Kleber 15 |
| 5 | RTV 3145 | 300°C | 72 Std. | $6 \cdot 10^{-6}$ | +0,79 % | 3,55 | 5,55 | geprimert; 24 Std. ausgehärtet; Bruch im Kleber 16 |
| 6 | RTV 3145 | 400°C | 24 Std. | $5 \cdot 10^{-5}$ | +5,35 % | b. Versuchsaufbau zerbrochen 11 | 0,3 | |
| 7 | X2-G-3488 DC | 200°C | 24 Std. | 10^{-6} | 0,53 % | 5,70 | 6,86 | geprimert; ausgehärtet; beim Zugversuch Bruch teilweise zw. Kleber u. Metall; b. Schervers. Bruch i. Kleber 17 |
| 8 | X2-G-3488 DC | 300°C | 24 Std. | $4 \cdot 10^{-6}$ | +1,49 % | 1,77 | b. Versuchsaufbau zerbr. | geprimert; ausgehärtet; Bruch im Kleber 18 |
| 9 | X2-G-3488 DC | 400°C | 24 Std. | 10^{-5} | +3,02 % | b. Versuchsaufbau zerbrochen 11 | b. Versuchsaufbau zerbrochen 11 | geprimert; ausgehärtet; Bruch im Kleber 18 |
| 10 | X2-G-3469 DC | 200°C | 24 Std. | 10^{-6} | 1,07 % | 20,9 | 13,5 | geprimert; ausgehärtet; Bruch im Kleber 18 |
| 11 | X2-G-3409 DC | 300°C | 24 Std. | 10^{-6} | +1,03 % | 6,26 | 5,01 | geprimert; ausgehärtet; Bruch im Kleber 18 |
| 12 | X2-G-3489 DC | 400°C | 24 Std. | 10^{-5} | +7,22 % | 6,25 | 8,76 | geprimert; ausgehärtet; Bruch im Kleber 18 |
| 13 | backer-Vergussmasse 22 | 200°C | 24 Std. | $2 \cdot 10^{-6}$ | 1,04 % | 1,26 | 0,62 | geprimert; ausgehärtet; Bruch nur teilweise i. Kleber |
| 14 | backer-Vergussmasse 22 | 300°C | 24 Std. | 10^{-5} | +3,4 % | b. Versuchsaufbau zerbrochen 11 | b. Versuchsaufbau zerbrochen 11 | geprimert; ausgehärtet; Bruch im Kleber. Da Ergebnisse für 300° sehr schlecht waren, erfolgte kein Versuch für 400°C 20 |
| 15 | RTV 560 | 200°C | 24 Std. | 10^{-6} | 0,31 % | 11,1 | b. Versuchsaufbau zerbrochen | geprimert; ausgehärtet; Bruch größtenteils im Kleber 21 |
| 16 | RTV 560 | 300°C | 24 Std. | 10^{-6} | +0,12 % | 0,5 | 0,5 | geprimert; gehärtet; Bruch nur teilweise im Kleber 19 |
| 17 | RTV 560 | 400°C | 24 Std. | $6 \cdot 10^{-6}$ | +1,9 % | 0,91 | 0,82 | geprimert; ausgehärtet; Bruch nur teilweise im Kleber 19 |

Key, Table 14

1- Number 2- Adhesive 3- Temperature 4- Experiment duration
 5- Pressure (torrs) 6- Loss of weight 7- Tensile test kp/cm^2
 8- Shear test kp/cm^2 9- Comments 10- Talcum and water glass
 11- Broken during set-up of experiment 12- Hardened $\frac{1}{2}$ day,
 break in adhesive; 13- Hardened 12 hours, break in the adhesive
 14- Hardened 24 hours; break in adhesive during tensile test; during
 the shear test there was a glass-like layer on which the sample
 broke 15- Primed, hardened 24 hours, break in the adhesive
 16- Primed, hardened 24 hours, break in the adhesive 17- Primed,
 hardened; during tensile test a break partially between adhesive
 and metal; during shear test break in adhesive 18- Primed, hardened,
 break in adhesive 19- Primed, hardened; break only partially in
 adhesive 20- Primed, hardened; break in adhesive; since the results
 were bad for 300° , there was no test at 400°C . 21- Primed, hard-
 ened, break mostly in adhesive 22- Wacker sealing compound

Aluminum samples glued with these adhesives in a climate box
 set up at a temperature of -60°C , $+100^\circ \text{C}$, $+150^\circ \text{C}$ and $+200^\circ \text{C}$ were
 subjected to shear and stress loads. In addition a second surface
 mirror (silver) was glued between two small aluminum blocks with
 XR-6-3489 and tested for tensile strength at room temperature.
 The results of these tests are recorded in Table 15.

TABLE 15 Tensile and Shear Strengths of Adhesives at
 Various Temperatures

| Adhesive | Temp. $^\circ \text{C}$ | Tensile strength kp/4 cm^2 | Shear strength kp/4 cm^2 |
|-------------|----------------------------|--|--------------------------------------|
| XR-6-3489 | + 100 | 86, 0 | 17, 7 |
| XR-6-3489 | + 150 | 43, 8 | 25, 6 |
| XR-6-3489 | + 200 | 42, 0 | 28, 7 |
| XR-6-3489 | - 60 | 250, 0 | 45, 5 |
| SilGel 2000 | + 100 | 35, 5 | 7, 0 |
| SilGel 2000 | + 150 | 23, 0 | 17, 2 |
| SilGel 2000 | + 200 | 23, 3 | 12, 0 |
| SilGel 2000 | - 60 | 205, 0 | - |

3.23 Changes in Transmission of Optical Adhesives by UV Radiation

To measure the transmission degradation of adhesives by UV an adhesive sample 6 mm thick was partially covered by a cover glass with a UV filter layer and irradiated. Before and after the UV radiation, the transmission was measured with a spectral photometer. The Zeiss spectral photometer was equipped with a double monochromator MM 12. A built-in UV fluorite prism assembly permitted measurements of 0.2 to 2.5 μ .

The UV radiation was accomplished with a UV standard lamp (250 W) from Philips (type no. 126066), a rectifier and built-in ignition coil from the company of Dr. Ing. Jovy, Leer/Ostfriesland (type ZUV 250 EB). The UV spectrum is formed of a continuum and lines and, especially in the very near UV region, deviates relatively little from the solar spectrum (Fig. 12). The manufacturer guarantees a constant yield for at least 2000 hours. To be certain the lamp was checked before and after the long usage. The dependency of the intensity on the distance between the lamp and measurement point was measured.

In order to make a logical comparison for the UV radiations of the stimulator radiation with the actual radiation from the sun, the concepts of equivalent UV solar constants and equivalent UV sun hours had to be defined.

Definitions:

- 1) An equivalent UV solar constant is that integral intensity between 0.2μ and 0.4μ which is equal to the integral intensity of the sun's radiation between 0.2μ and 0.4μ (near UV) outside the earth's atmosphere (near the earth = 1 AE distance from sun).
- 2) An equivalent UV sun hour is that integral energy flux between 0.2μ and 0.4μ which equals the energy flux of the sun integrated in one hour (between 0.2μ and 0.4μ) outside the earth's atmosphere.

As one can deduce from Figure 12, during utilization of a wave length smaller than 0.4μ for the upper limit of the UV region with a UV standard lamp a larger UV constant and thus (with long-term radiation) more equivalent sun hours than at a maximum wave length of 0.4μ . If one takes, for example, 0.3μ as the upper wave length limit, an equivalent UV solar constant larger by about a factor of four results for the UV standard lamp.

The calibration of the UV lamp in UV solar constants was accomplished in the following manner: The density of radiated power of the lamp at a 1 m distance between 200 mm and 400 mm was known. The multiplication factor of the power for shorter distances was derived by the relative measurement of a solar cell (Siemens model IV). Multiplication of the power density at 1 m distance with

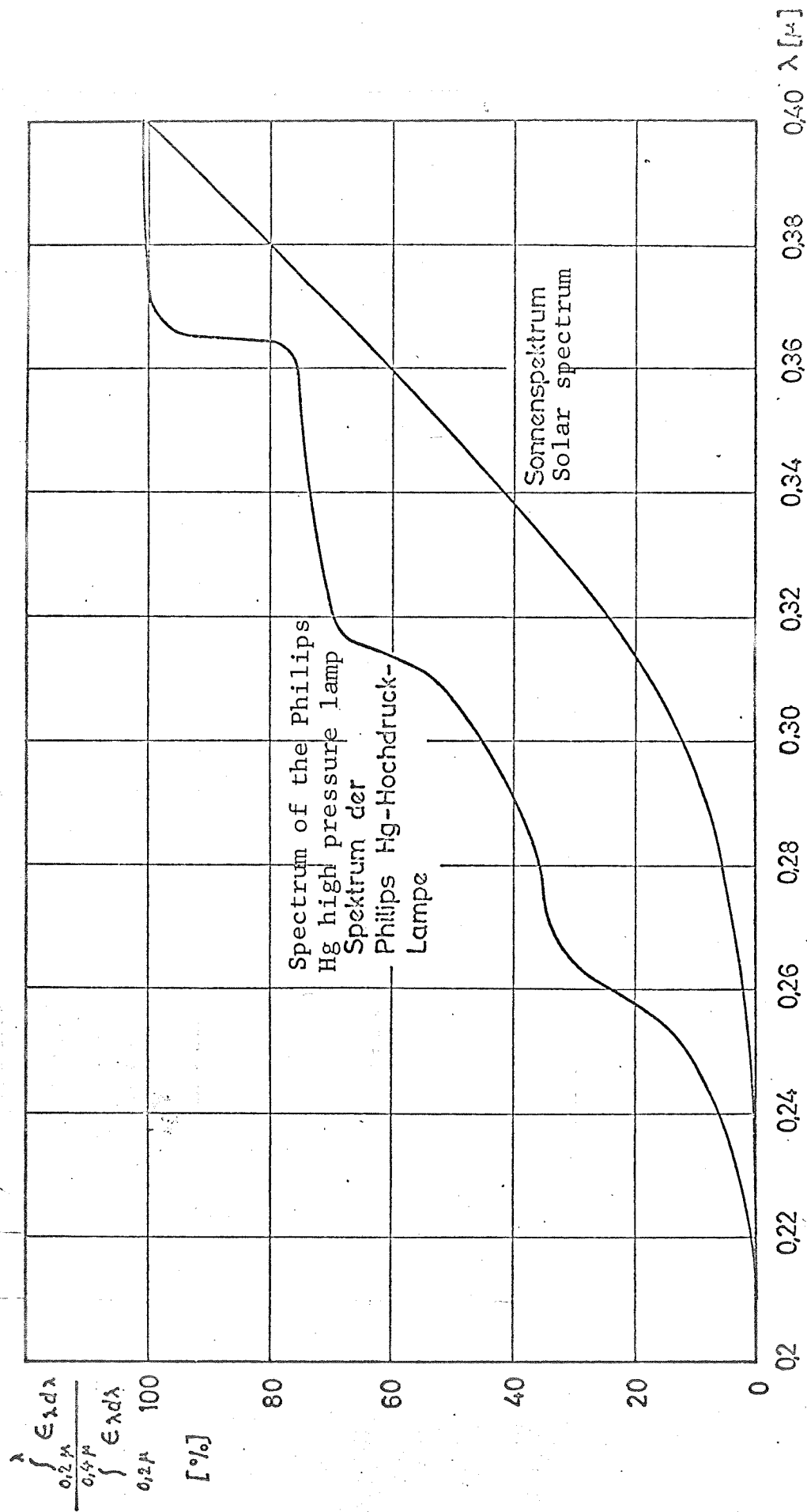


Fig. 12 UV spectrum of the UV standard lamp (Philips model 126066, 250W)

this factor and division by the actual radiated power density of the solar radiation near the earth (1 AE sun distance) between 200 mm and 400 mm produced the calibration of the radiated power density in equivalent solar constants.

The irradiation of the adhesive proceeded in air over 100 hours at 9.5 UV solar constants. Since no significant UV degradation of the adhesive was expected for a 25 μ thick adhesive, an adhesive thickness of 6 mm was selected. The adhesive sample (40 x 40 x 6 mm) was partially covered by a cover glass with a UV filter layer and irradiated, whereby the sample heated up. The transmission curves before and after the irradiation, measure at points with and without a cover glass, are shown for adhesive type XR-6-3489 in Figure 13. It is apparent that the transmission loss is small and, thus, that it is small enough to be ignored for the 25 μ thick adhesive layer in the solar cell module. (Of course, a conversion of the transmission loss from a 6 mm sample to a 25 μ layer by simply dividing by 240 is not correct since the adhesive does not degrade homogeneously, but breaks down chiefly on the radiation side). However, the unprotected part of the sample shows a very high degradation (Figure 13) which cannot exclusively be attributed to clouding, but is caused by the surface becoming crusted (Figure 14). Behind the cover glass, though, the adhesive remained clear and smooth.

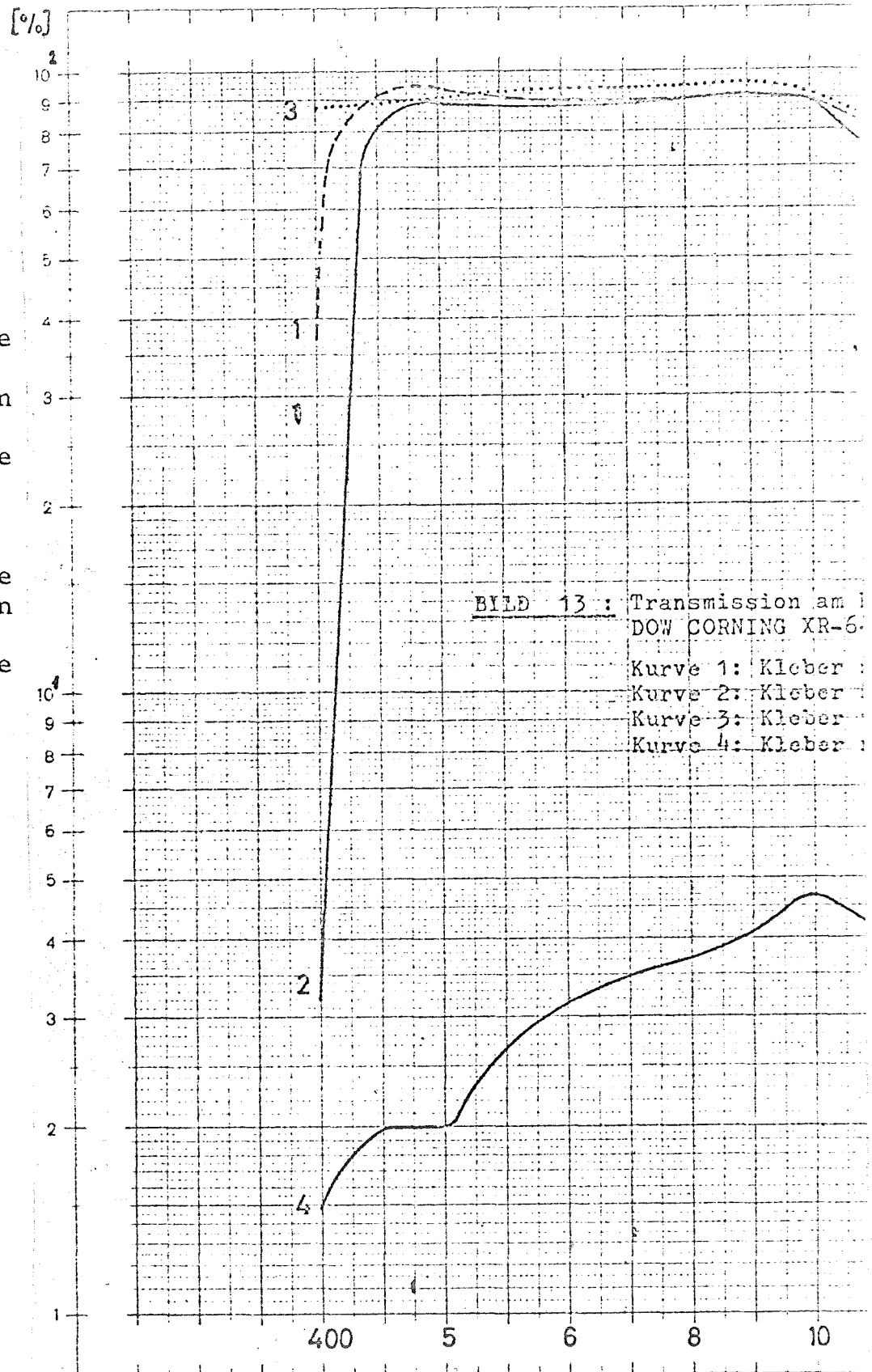
Fig. 13 Transmission in the adhesive before and after UV irradiation
Dow Corning XR-6-3489 (Figure continued on p.41a)

Curve 1: Adhesive
with cover glass
before irradiation

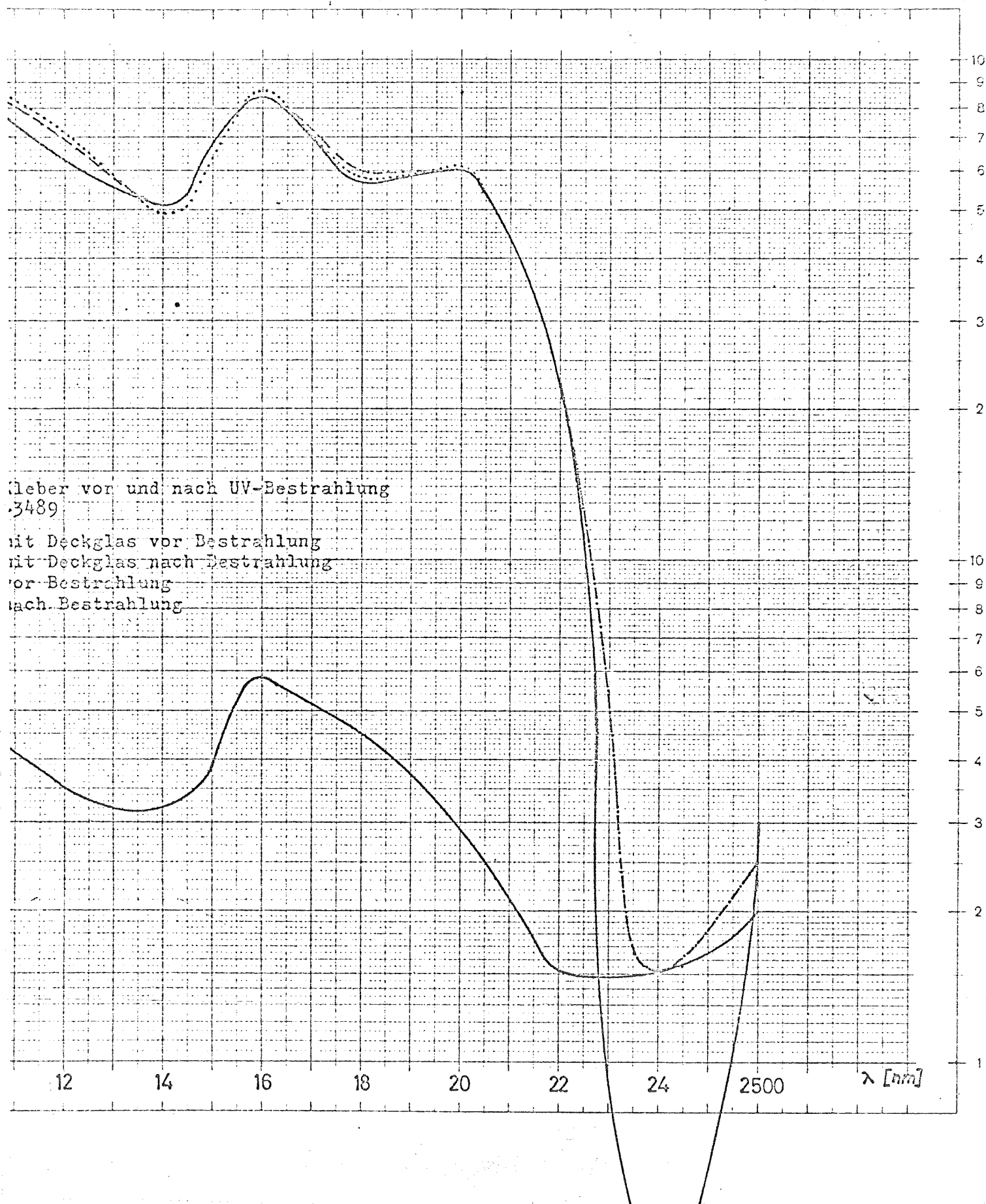
Curve 2: Adhesive
with cover glass
after irradiation

Curve 3: Adhesive
before irradiation

Curve 4: Adhesive
after irradiation



One axis logarithmically divided from 1 to 100, unit 100 mm, the other in mm.



Such a crust was only encountered for UV irradiation in air with an unprotected adhesive. It did not occur for UV irradiation in a vacuum (1000 h xenon lamp at 1 solar constant or during long-term testing in a thermal vacuum (without irradiation)).

3.24 Cover Glass Assembly

For the usual cover glass assembly the adhesive XR-6-3489, which proved to be the best for high temperature applications, exhibited certain difficulties with the reproducibility of the adhesive thickness (dosage at higher viscosity) and the leakage behavior. Thus, a new method was developed for bonding the cover glass to solar cells, and a device was built which made it possible to bond together cover glass and cell without having surplus adhesive leak over the glass surface and which assured a sufficiently reproducible adhesive layer thickness. A cover glass is set into a positioning device and held tight by means of a suction stub. A stamp applies the required amount of adhesive to the cover glass (Fig. 15) A bell is set over the adhesive covered glass and evacuated (Fig. 16). Thereby, the already degassed adhesive is again degassed and flattened on the glass. Furthermore, a solar cell is set into a mounting in another glass bell (to which the silver mesh lug on the grid strand is already welded (Fig. 16). The bell over the cover glass is pressurized, removed and replaced by the

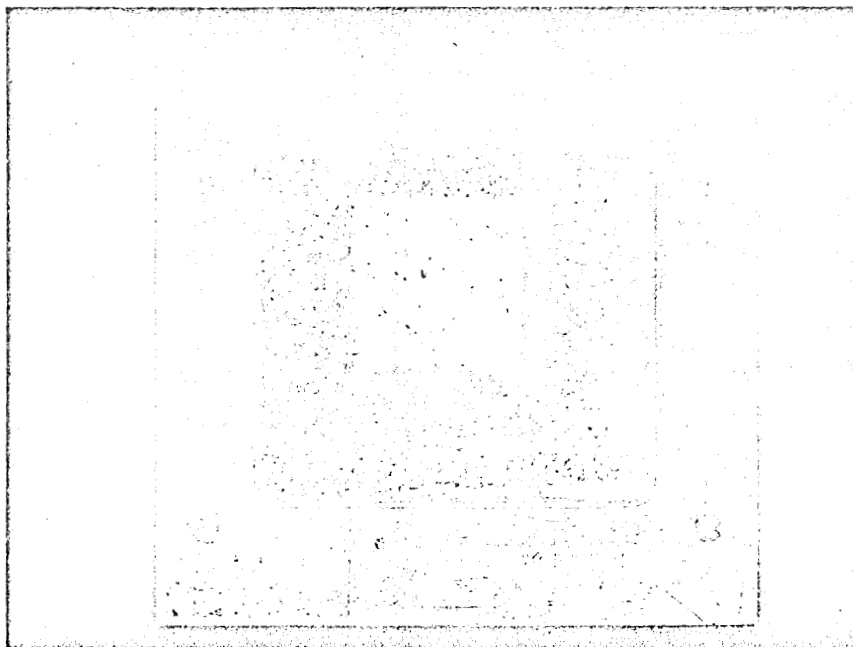


Fig. 14 Adhesive sample (type XR-6-3489) after UV irradiation

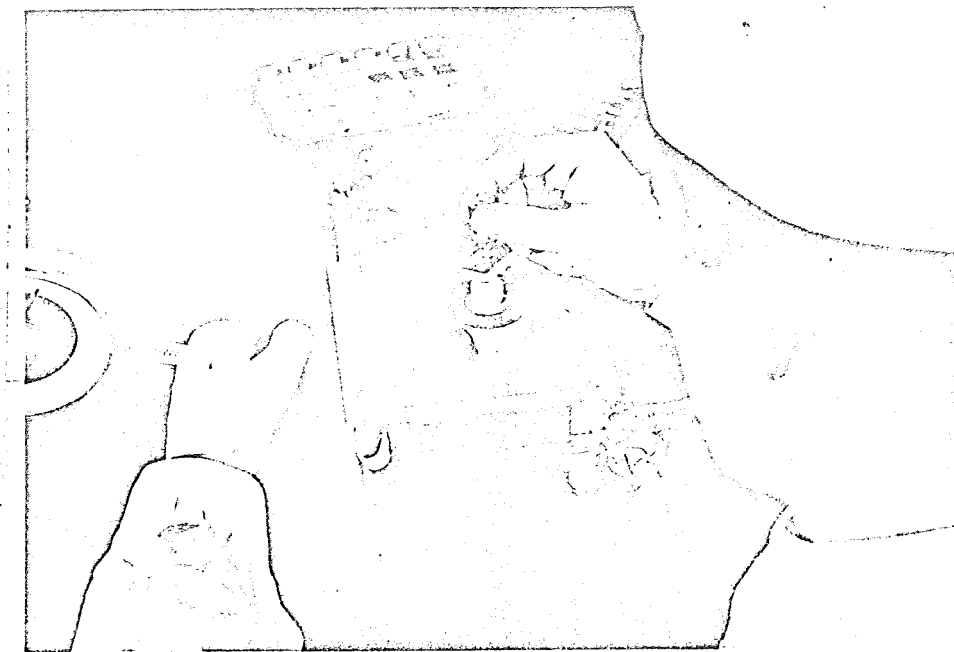


Fig. 15 Coating the cover glass on the suction stub with adhesive

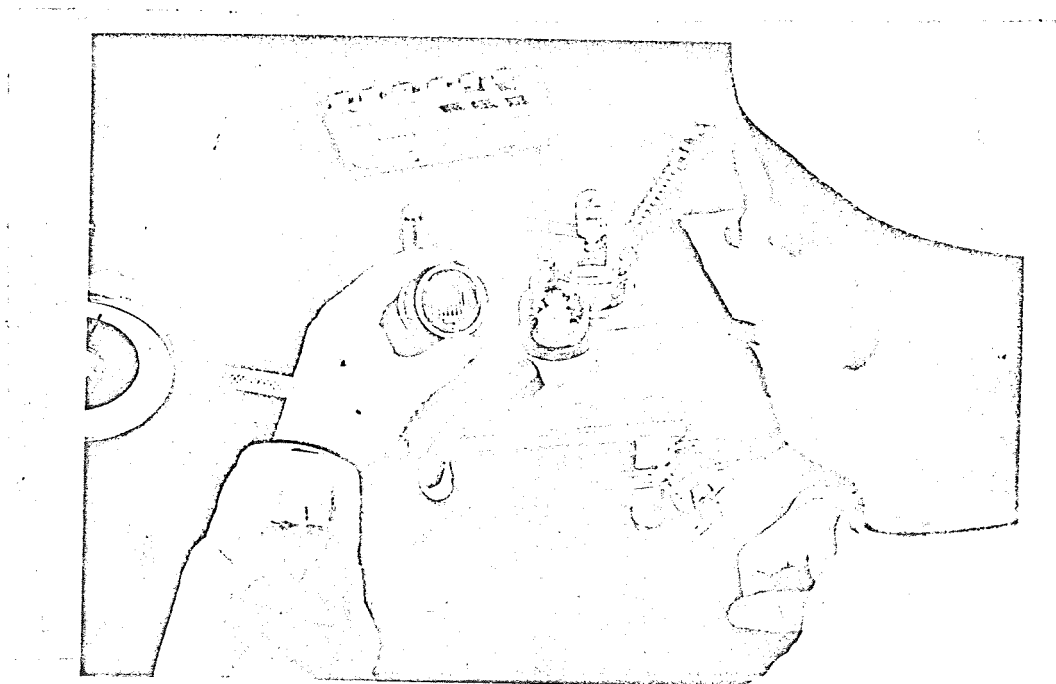


Fig. 16 Evacuation and spring mounting for the solar cell

bell with the solar cell. After the evacuation of this bell the solar cell is set down, free of bubbles, on the cover glass prepared with adhesive by means of a universal wall entrance (Fig. 17). After pressurizing the apparatus the cell fitted with a cover glass is put in a mounting and heated by an infrared emitter to harden the adhesive (Fig. 18). The thickness of the layer produced by this method amounts to $25 \pm 5\mu$.

3.3 Non-optical Adhesive

Various adhesion techniques with non-optical adhesives were to be investigated. Preceding tests on cover glass bonds with optical adhesives permit one to say that at higher temperatures (above 200°C) most optical adhesives are unsuitable with respect to stability and transmission.

According to the original demands for the Helios experimental program, though, the solar cell modules were to endure high shock temperatures. For this reason, correct, new adhesion techniques had to be found.

The possibility offered itself for the solar cell of utilizing the silver grid surfaces, which as a matter of course do not effect the effective light surface of the solar cell, as adhesive surfaces. Thus, a method had to be found to wet the silver grids with adhesive so that no other surface parts would be contaminated with the opaque high temperature adhesive. For this, a covering template was used



Fig. 17 Applying a solar cell to the cover glass

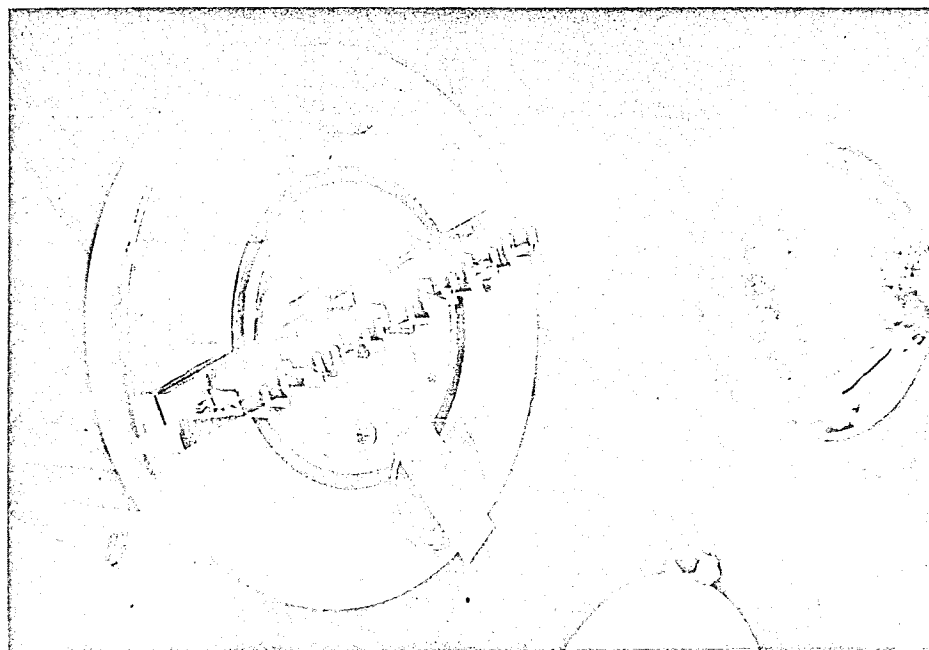


Fig. 18 Hardening the cover glass adhesive by IR irradiation

which possessed openings through which the adhesive comes to meet the silver grid. In contrast with techniques with transparent adhesives which cover the entire surface of the solar cell, for the partial adhesion attachment of the cover glasses to the metal grids a primer can be used. The reduced adhesion surface is thusly compensated by a higher specific cohesiveness.

In order to avoid the expense and delay of a completed adhesive spraying apparatus which can spray all sorts of adhesives (most varying viscosities), a commercial adhesive in spray cans was tried. According to detailed information from the leading producers, it was found out that the special high temperature adhesive we wanted was not available in spray cans. Therefore, we fell back on a common adhesive delivered by the 3M Company in spray cans (type: spray adhesive 77).

The basic determination that the experiments were to make, was not affected by this since with the proper application the specified silicon adhesive could also be used in the spray technique. The adhesive was sprayed on the solar cell grid through templates and finally stuck to a cover glass after the emplate was lifted off. Vaporization templates for the Siemens solar cell grid served as our templates. To measure the separation strength a spring scale with a maximum reading of 2.5 kp was selected. The underside of the solar cell was glued with rapid adhesive, corresponding to the

load direction (shear or tensile test) to the aluminum surfaces designed for this. "Separation plates" corresponding to shear or tensile loads were glued to the cover glasses.

Table 16 shows the result of the separation tests. Apparently, there were good values for the adhesive stability with the specially used adhesive. No leakage problems appeared during the spray technique since the positioned template did not touch the surface of the cells.

3.4 Cover Glass Assembly by Thermodiffusion

A way to connect the solar cell and cover glass without the use of an organic adhesive was sought. On the basis of the results of primary investigations on thermodiffusion (Ref. 1), it was expected that this type of connection could also be used for attaching cover glasses to solar cells. To this end the connecting parts must be bonded under pressure and at high temperature. The temperature needed for the connection lies at ca. half of the melting temperature of the metal to be connected. In order to connect the cover glasses with the cells a +Ti — Ag layer was coated on the cover glasses (at Siemens). For the first experiments the glasses were coated on the entire surface and untempered cells were used. Later the grid structure with two additional zones of ca. 2 mm² was coated to the cell and cover glass with a modified template (at Siemens) (Figures 19, 20). The additional coating zones somewhat eased

TABLE 16 Separation Tests on Partial Cover Glass Bonding (Spray Adhesive 77 from 3M

| Test No. | Spray time | Surface drying time before fixing min | Complete drying time after fixing min | Drying temperature | Shear strength P_s (kp) | Stress strength P_z (kp) | Comments |
|----------|------------|---------------------------------------|---------------------------------------|--------------------|---------------------------|----------------------------|--|
| 1 | 2 | 1 | 2 | 60 | 0,5 | - | Normal cleaning with Per |
| 2 | 2 | 1 | 2 | 60 | - | 0,3 | |
| 3 | 2x 0,5 | 1 | 5 | 60 | 2,3 | - | |
| 4 | 2x 0,5 | 1 | 3 | 40 | - | 1,9 | Cleaning with 80°C hot Per, ultrasonic |
| 5 | 1x 0,5 | 1 | 3 | 40 | - | 1,8 | |
| 6 | 1x 0,5 | 3 | 5 | 50 | 2,0 | - | |
| 7 | 1x 0,5 | 3 | 3 | 60 | - | 2x 2,4 | Cover glass breakage |
| 8 | 1x 0,5 | 3 | 3 | 60 | 4x 2,4 | - | Cover glass broke, and silver grid became disconnected |
| 9 | 1x 0,5 | 3 | 3 | 60 | 2x 2,4 und 1x 2,2 | - | Breakage |
| 10 | 1x 0,5 | 3 | 3 | 60 | - | 2,4 | Cover glass broke and silver grid became disconnected |

In comparison: Gluing of the entire surface with RTV 602 produced ca. 4 kp stress or shear strength on the 4 cm² cells.

the positioning difficulties, which were caused by the very small grids.

The necessary diffusion temperature was reached in an electrically heated oven. The cover glass and solar cell were placed in this oven such that they were pressed together by a weight on top of them. The pressure was produced by a weight which was transmitted to the pressure plate by ceramic tubes (Fig. 21).

In order to prevent an oxidation of the silver surface at the necessarily high diffusion temperature, the thermodiffusion was run in a buffer gas atmosphere (argon, nitrogen). In order to prevent great losses of heat the gas pressure was kept at ca. 1 torr. After heating the oven ca. 30 min. to the desired temperature (between 400° C and 600° C), the temperature was maintained for ca. 30 min. then cooled in ca. 30 min. The pressure between the cover glass and solar cell amounted to between 2 kp and 5 kp. The separation tests produced quite varied adhesion between the cell and the glass (0-23, 4 kp, cf. Table 17). The pull was here perpendicular to the cell and/or glass surface. For this, the samples were glued between aluminum blocks with clamps. For the cell with the highest separation strength (23.4 kp) the stress was held for 3 min. at 20 kp. Figures 19 and 20 show the cell and cover glass after the separation test. (Adhesion occurred at the solder strand since for these special tests no cover glasses with holes for later soldering were used.)

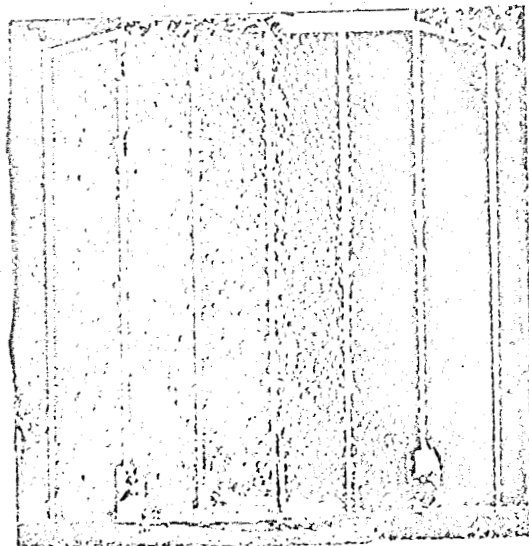


Fig. 19 Cell after being torn from a cover glass fastened by thermodiffusion

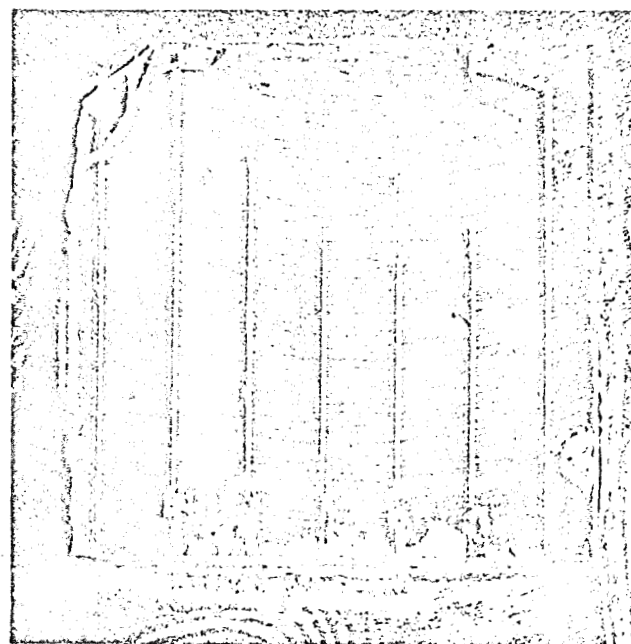


Fig. 20 Cover glass after being torn from a cell fastened by thermodiffusion

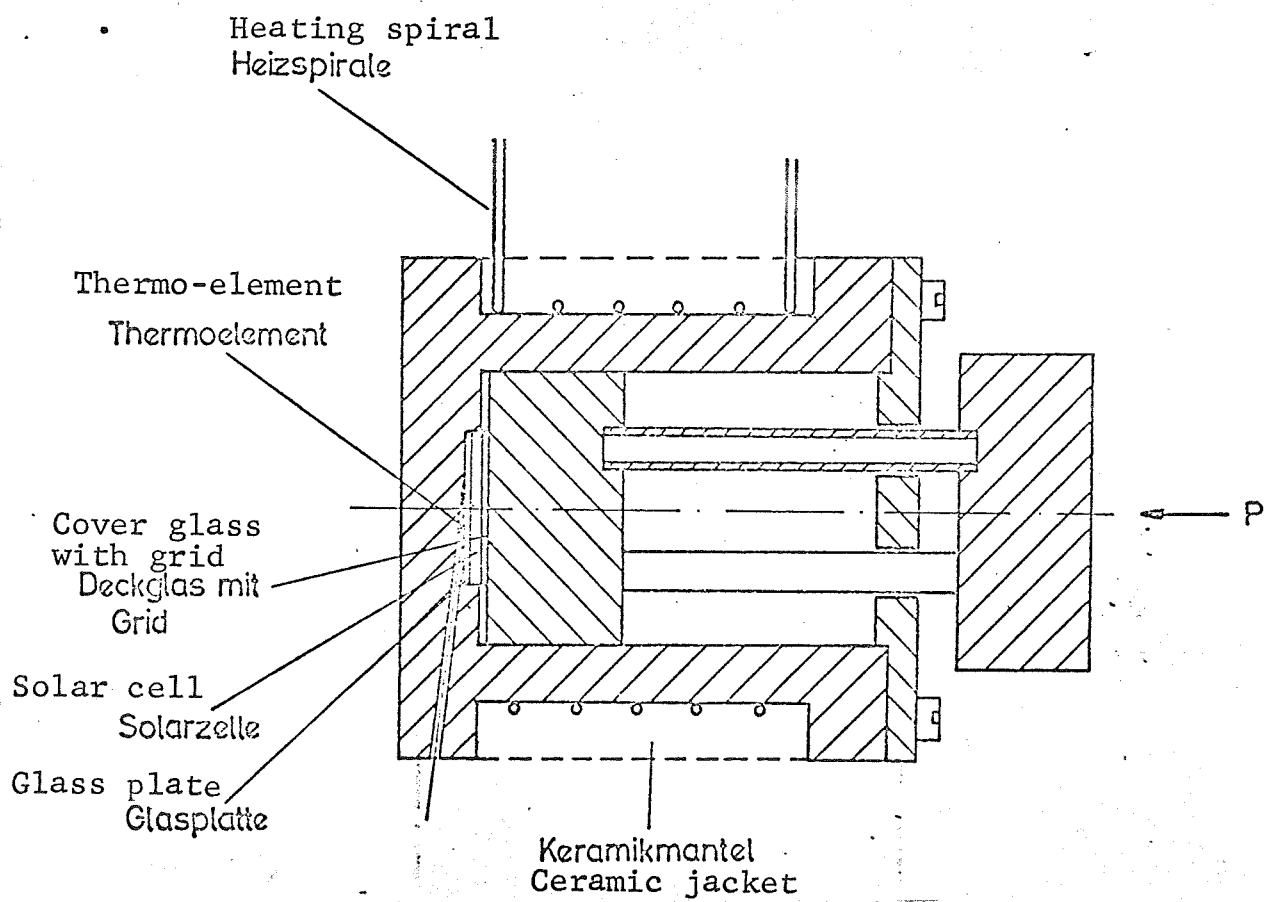


Fig. 21 Oven for connecting cover glass and cell by thermomodification

TABLE 17 Adhesive Stability of Thermodiffusion Bonds

| Test | Pressure kp | Temperature °C | Separation strength, kp for 4 cm ² | Length of diffusion min. | Comments |
|------|----------------|-------------------|---|--------------------------------|---------------------------------|
| 1 | 5 | 500 | 8, 6 | 30 | completely silvered glass |
| 2 | 2 | 420 | 0 | 30 | " |
| 3 | 2 | 400 | 0 | 30 | " |
| 4 | 5 | 445 | 0 | 30 | " |
| 5 | 2 | 500 | 0 | 30 | " |
| 6 | 2 | 550 | 0 | 30 | " |
| 7 | 2 | 550 | 0 | 30 | " |
| 8 | 2 | 600 | 0 | 30 | " |
| 9 | 5 | 500 | 2 | 30 | " |
| 10 | 5 | 550 | 2, 5 | 30 | " |
| 11 | 5 | 400 | 2 | 30 | " |
| 12 | 5 | 400 | 0 | 30 | " |
| 13 | 5 | 450 | 2 | 30 | " |
| 14 | 3 | 400 | 4, 3 | 30 | Cover glass with Ag grid |
| 15 | 4 | 500 | 0 | 30 | " |
| 16 | 5 | 600 | 6, 8 | 30 | " |
| 17 | 5 | 500 | 23, 4 | 30 | " |
| 18 | 4 | 400 | 9, 8 | 30 | " |
| 19 | 3 | 600 | 5, 7 | 30 | " |
| 20 | 3 | 500 | 0 | 30 | " |
| 21 | 5 | 400 | 0 | 30 | " |
| 22 | 4 | 600 | 17, 3 | 30 | " |

Basically, the experiments showed that a good connection is possible by thermodiffusion, but that still other research is necessary. In particular, the accuracy of positioning, which is important in the adhesive stability, must be increased, and the method must be made more practicable.

3.5 Losses through Non-optimal Index of Refraction Transitions between the Cell and Cover Glass

Because of the poor optical transition between the cover glass and solar cell, the cover glass connection by thermodiffusion or with a non-optical adhesive causes a lessening of the degree of effect of the cell. At Siemens the quantum yield of solar cells was measured, without cover glass, with glued cover glass and with a non-attached cover glass lying on the cells (Figures 22 and 23). Table 18 shows the corresponding short-circuit currents and their degradations (Power degradations are somewhat smaller).

TABLE 18 Cell Degradation by Cover Glasses

| | Short-circuit current (mA) Kurzschlußstrom (mA) | | |
|-----------|--|--|---|
| | ohne Deckglas without cover glass | with glued cover mit geklebtem Deckglas XR-6-3489 | with loose mit lose Deckglas cover glass |
| 270 Z 138 | 142,3 | 137,8 (- 3,2 %) | - |
| 270 Z 133 | 141,7 | 138,0 (- 2,6 %) | - |
| 270 Z 128 | 140,9 | 137,2 (- 2,6 %) | - |
| 270 Z 151 | 140,4 | 137,1 (- 2,3 %) | - |
| 259 T 177 | 138,4 | | 130,1 (- 6,0%) |

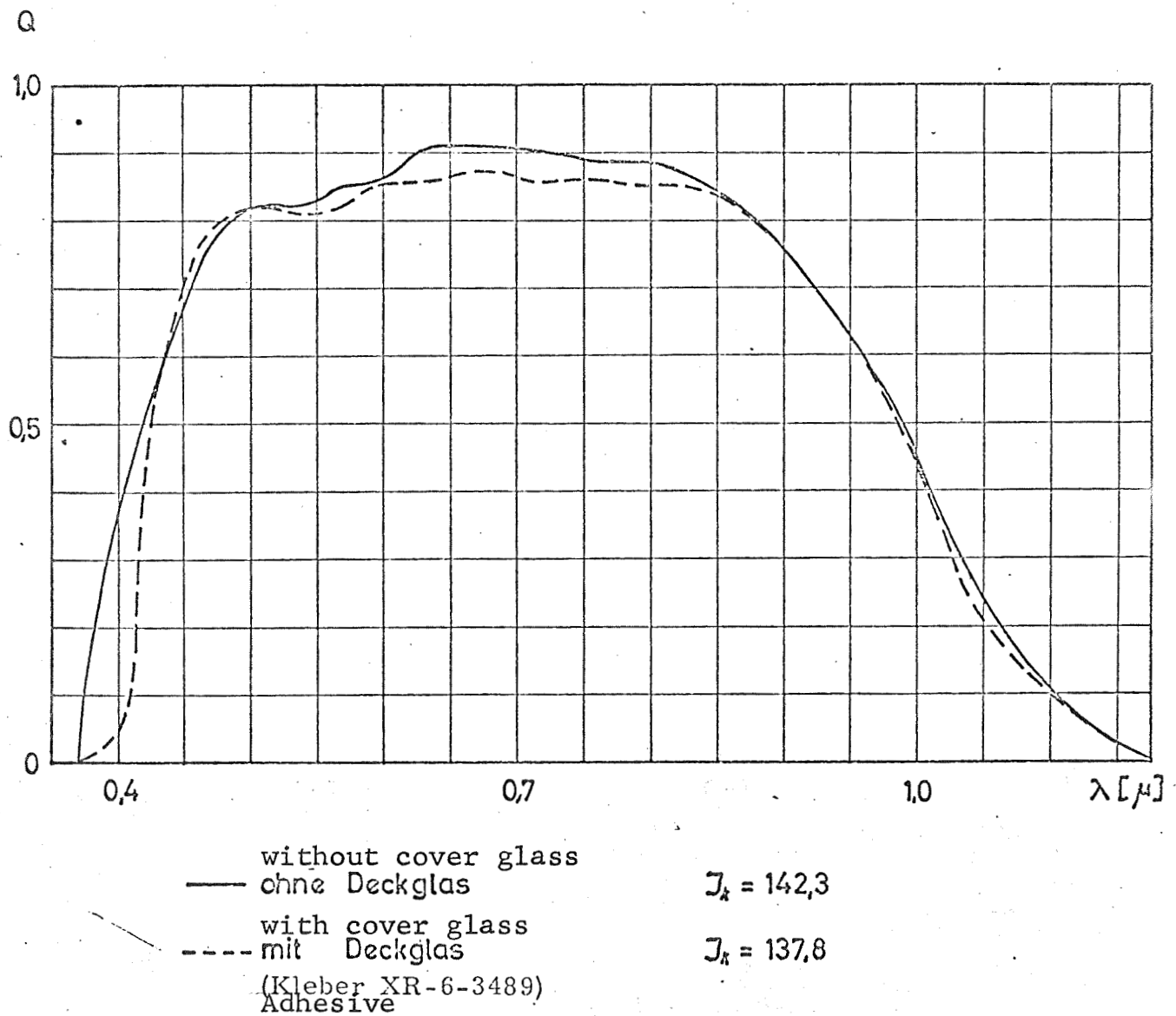


Fig. 22 Quantum yield of a solar cell with and without glued cover glass

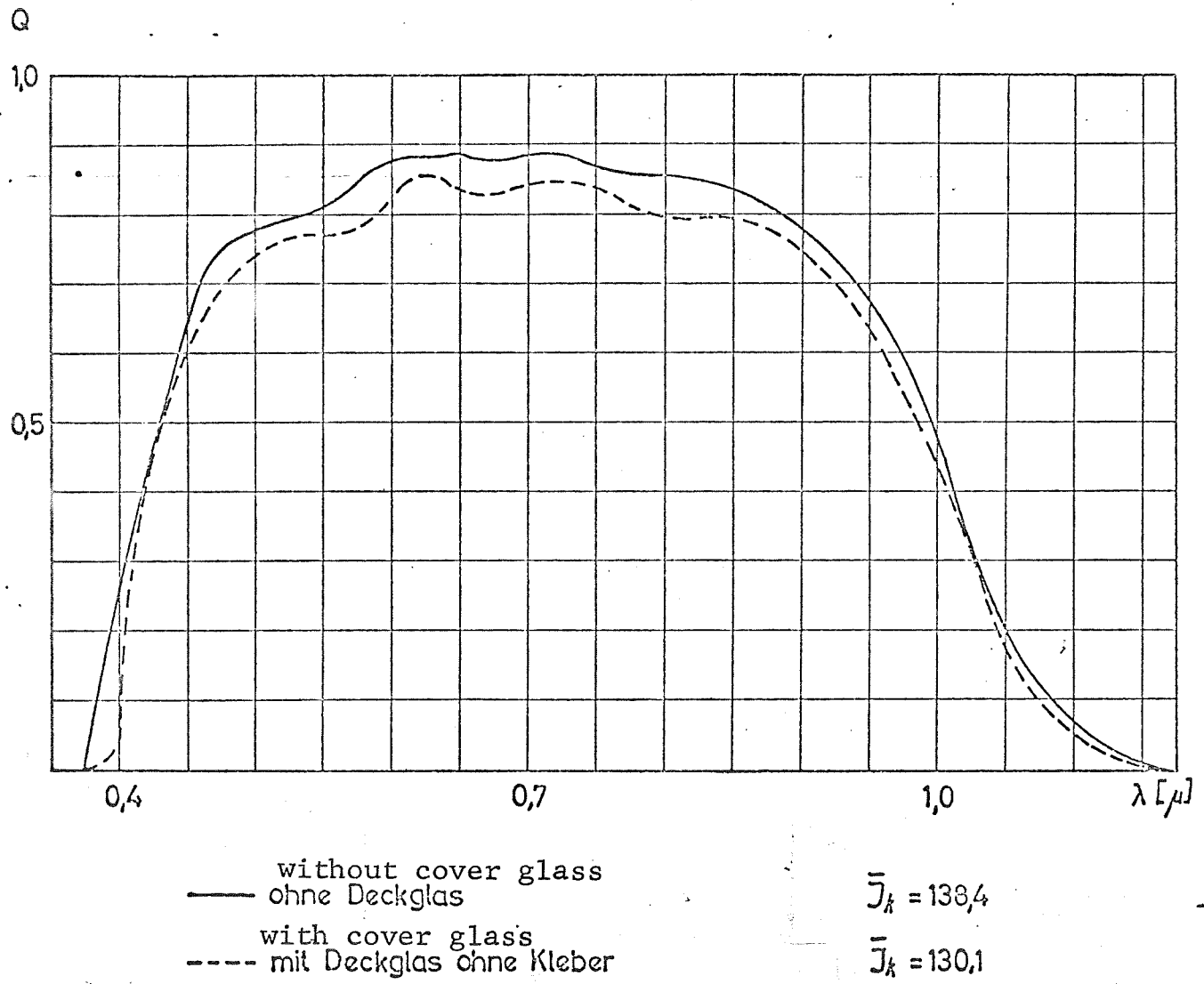


Fig. 23 Quantum yield with and without a loosely positioned cover glass

4. HIGH TEMPERATURE FOILS

4.1 Selection of Foils

The following foils were considered as supporting foil for the solar cells, for the electrical return circuit and as insulating foil:

- GfK (Mica Corporation)
- Milclad (Riegel)
- Kapton (Riegel)

The selection criteria for these foils are:

- high temperature stability
- good vacuum stability
- good isolation characteristics
- suitability for copper lining
- good adhesive base for bonds
- little weight

The foils used were partially already delivered from the producer, a copper-lined connection foil.

4.2 Tests on Foils

The foils just cited were set out in a temperature between 200° and 450° C at a pressure of from 10^{-5} to 10^{-6} torrs. Table 19 shows the weight losses.

GfK foil survives 200° C without large weight loss, at 300° a large loss of weight already occurs. At 400° C the Cu foil separated

TABLE 19

Weight Losses of Connection Foils in the Thermal Vacuum

| Gfk copper-lined 20 μ Cu, 70 μ GfK | | | |
|---|------------|---------------------------|----------|
| 24 | hours at | 200 $^{\circ}$ C | 0,68 % |
| 72 | " | 300 $^{\circ}$ C | 10,47 % |
| 72 | " | 300 $^{\circ}$ C + 24 | |
| | " | 400 $^{\circ}$ C | 13,36 % |
| 24 | " | 200 $^{\circ}$ C | 0,77 % |
| +72 | " | 300 $^{\circ}$ C | + 9,69 % |
| +24 | " | 400 $^{\circ}$ C | + 2,24 % |
| Milclad copper-lined 35 μ Cu, 76 μ Milclad | | | |
| 24 | hours at | 200 $^{\circ}$ C | 0,6 |
| 24 | " | 250 $^{\circ}$ C | 1,97 % |
| 6 | " | 300 $^{\circ}$ C | 4,65 % |
| 6 | " | 350 $^{\circ}$ C | 22,5 % |
| 5 | Minutes at | 400 $^{\circ}$ C | 17,88 % |
| 5 | " | 450 $^{\circ}$ C | 26,92 % |
| Kapton foil copper-lined 35 μ Cu, 76 μ Kapton | | | |
| 24 | hours at | 200 $^{\circ}$ C | 0,8 % |
| 24 | " | 200 $^{\circ}$ C and 36 | |
| | | hours at 300 $^{\circ}$ C | + 3,3 % |
| 24 | hours at | 300 $^{\circ}$ C | + 3,1 % |
| 410 | " | 240 $^{\circ}$ C | 1,6 % |

from the GfK foil since this latter had almost lost all the epoxide and consisted almost solely of a glass fiber structure. Milclad foil contracts already at 200 $^{\circ}$ C and carbonizes at 450 $^{\circ}$. Cu-lined Kapton foil proved to be very stable. Up until 200 $^{\circ}$ C

no foil changes could be determined. The 0.8% weight loss which occurs seems, apparently, to be caused by weight loss of the adhesive between copper and Kapton. At 300°C bubbles formed in the copper, which could be attributed to a vaporization of the adhesive. The Kapton foil itself showed no change at 300°C. The cause of this limited temperature stability is the fact that, up to the present, commercially prepared Kapton - Cu connection foils have always come with polyester adhesive layers. (Cu - Kapton connection foils without intermediary adhesive layers are under development). Since type XR-6-3489 (Ch 3) was found to be a thermally very stable adhesive, the production of Cu-Kapton foils with this very adhesive suggested itself. Good results were achieved when a thin layer of adhesive XR-6-3489 was applied to a sand-blasted 25 μ Kapton foil; annealed, purified 50 μ Cu foil was pressed on, degassed and then brought into the air to harden in a pressed condition at 150° C (for ca. 30 min.). This self-made type of connection foil was later used for the test module and functioned well in the thermal transit time test (180° C, 260 h, 10⁻⁶ torr) cf. Ch. 5 and 6.

4.3 Process for Fabrication of Modules

After determining the form of the current return circuit, the conductor channels were photolytically etched on the various types of connection foils. After bonding an insulation foil

(non-interlaced Mylar or Kapton foil) over the current return circuit by means of a hot press on the Cu side, the solar cells welded together in a module are bonded in a vacuum. The electric connection between the current return circuit and the module is made by welding the silver mesh to the module ends with the Cu conductor channel, see Figure 24.

4.4 Conclusion

Kapton appears to be the most suitable foil for the production of the module. At temperatures under 200° C the marketed Kapton - Cu connection foil (cf. 4.2) utilizing the silicon adhesive XR-6-3489. Detailed experiments for a suitable production process for larger surfaces have not been undertaken.

5. MODEL MODULE

5.1 Module Construction (Production Process)

Previously, the following successive steps served in building the module: checking input of the solar cells, placing the cells together in pairs (matching), soldering the submodules to modules, cover glass bonding (simultaneous for all cells of the module), measuring the module, bonding the carrier foil with the current return circuit to the module. The leakage of superfluous adhesive on the cover glasses, especially with the selected high temperature adhesive XR-6-3489, could not be prevented. Also, because an

incorrect mounting of a cover glass, the entire module had to be repaired. In order to prevent this a new process was developed for bonding the cover glass. The resulting fabrication series for the module is as follows:

- input check on the solar cells
- welding silver mesh to the grid strands
- bonding of cover glass (to individual cells)
- measurement of the cells covered with a cover glass
- sorting the cells after the short-circuit current
- matching the module cells
- welding together to a module (welds on the back sides of the cells)
- measurement of the module
- welding the end connectors of the module to the current return circuit.

The device mentioned for the bonding of the cover glass and the resulting fabrication series for the module had significant advantages over the previously used module fabrication.

- lessening of the leakage problem of adhesive (thus, no difficulties with cleaning)
- the adhesive layer thickness is thin (25μ) and more easily reproduced ($25 \pm 5\mu$)
- no difficulties in positioning while bonding the cover glass

- no difficulties when replacing cells (on account of glass or cell breakage during the cover glass assembly)
- The cells were measured and put together after the cover glass bonding. This eliminated changes in the short-circuit current by the cover glass bond (match losses)
- The rate of breakage in solar cells during production of the module was decreased.

5.2 Construction of Model Modules

The following summary reproduces the individual components of a solar cell module whose characteristics permit the application at temperatures over 200° C.

The series repeats the steps of the construction:

1. Welded solar cells (Ag mesh: 2A65-6/0. Exmet Corporation)
2. Cover glass (Heräus) and adhesive (XR-6-3489 Dow Corning)
3. Adhesive (XR-6-3489 Dow Corning) and Kapton - Cu supporting foil (bonded with XR-6-3489 Dow Corning, cell distance 0.3 mm)
4. Adhesive (XR-6-3489 Dow Corning) and Mg sheet as support (AZ31 with Dow 17 corrosion protection layer, 0.4 mm thick).

Several modules with 12 cells were built from the components mentioned above for demonstration purposes (Figures 24 and 25); further, 6 modules with 4 solar cells each were built for test purposes (Figure 27) and a module with 2 solar cells and 2 second surface mirrors was produced for heat balance measurements (Fig. 28).

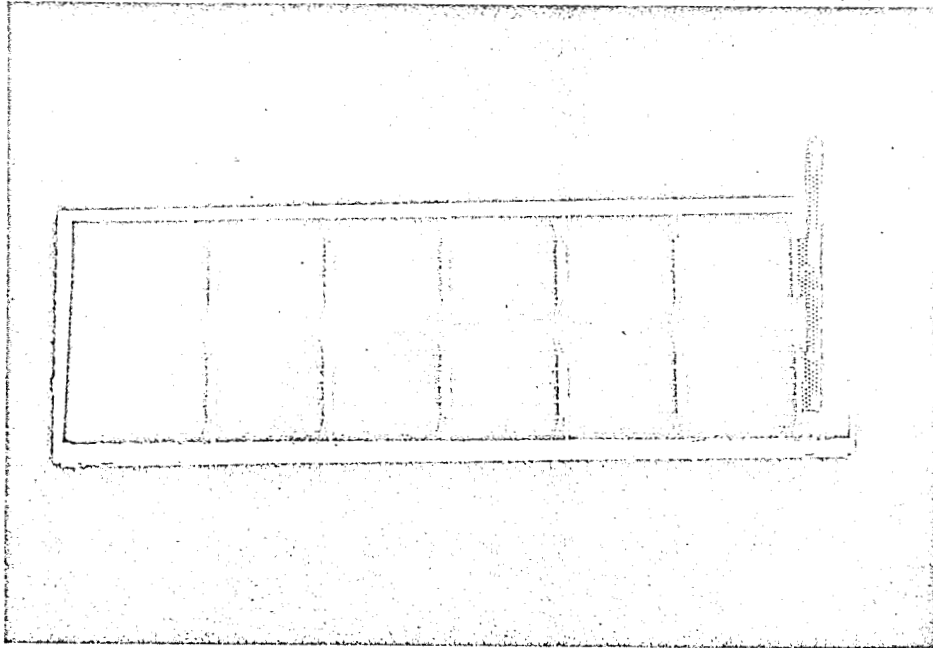


Fig. 24 Module with welded solar cells (front side)



Fig. 25 Welding module (back side)

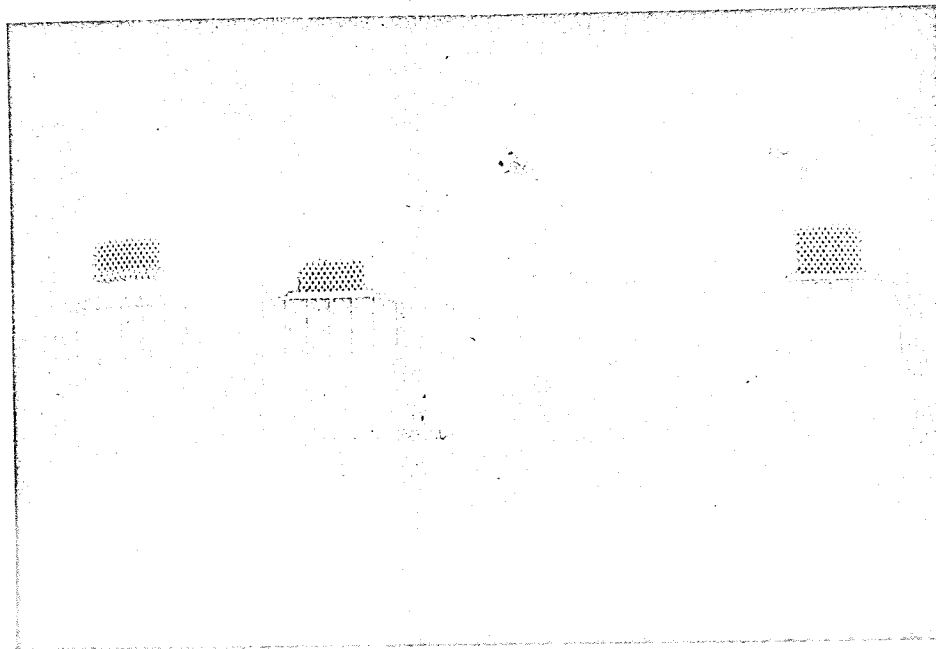


Fig. 26 Intermediary stages in the construction of a glass-covered solar cell

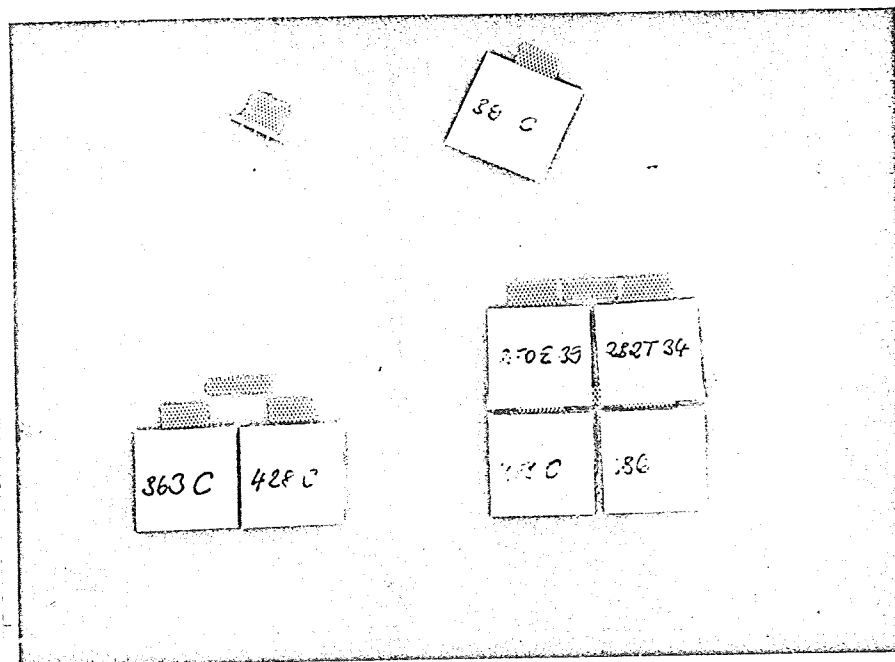


Fig. 27 Construction of a test module

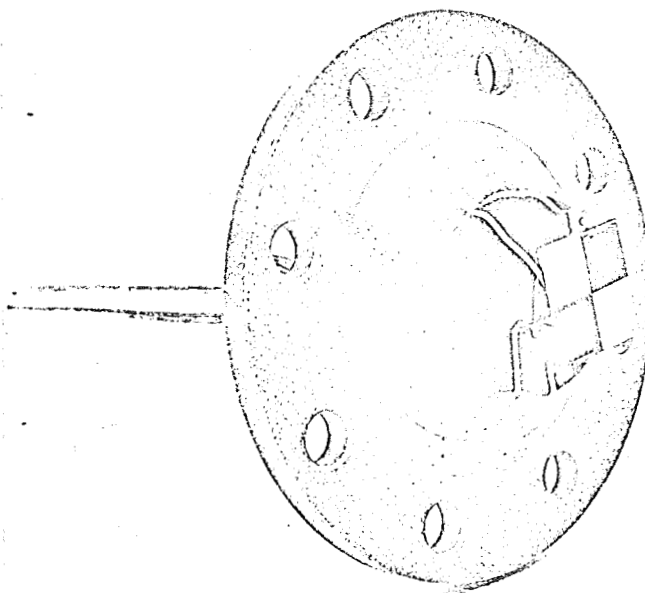


Fig. 28 Module with 2 solar cells and 2 second surface mirrors for the heat balance measurement

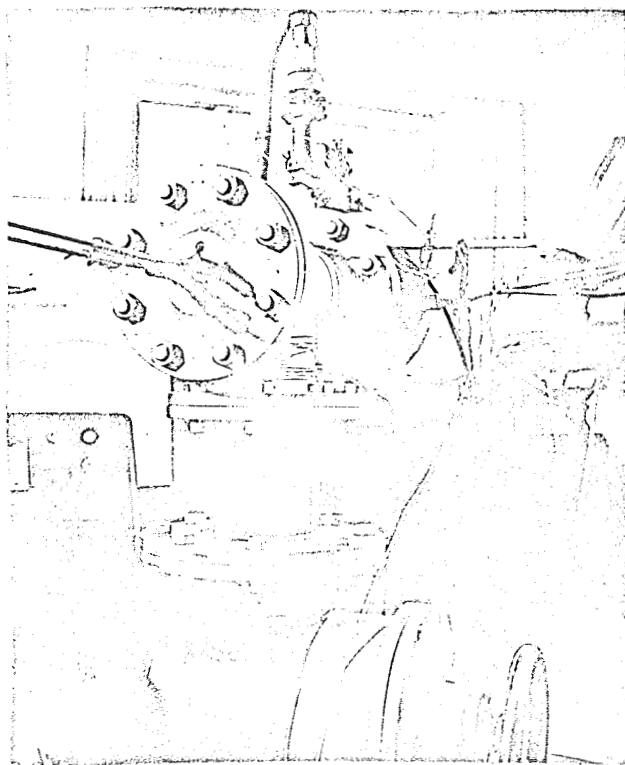


Fig. 29 Test chamber for the heat balance measurement

Figure 26 illustrates the steps for the construction of the glass-covered solar cells as they are put together in a module. In Figure 27, moreover, one can see the behavior for the direct connection of two cells during welding.

5.3 Tests on Model Modules

The following tests were made on solar cell modules of 4 cells each:

- climate test
- thermal vacuum
- thermal shock
- vibration

The electrical characteristics (short-circuit current J_K , no-load voltage U_L of the test module were measured at the standard measurement location (W-lamp with momentary illumination of the module by means of a movable slit diaphragm to avoid temperature changes) before and after the tests.

5.31 Climate test

The specifications are reproduced in Table 20.

After the test the module showed no mechanical or visual changes. The electrical properties (short-circuit current I_K , no-load potential U_L) remain the same.

Before the test: $I_K = 226.5 \text{ mA}$, $U_L = 1.134 \text{ V}$

After the test: $I_K = 226.3 \text{ mA}$, $U_L = 1.134 \text{ V}$

TABLE 20 Climate Test

| Running time (h) | Temp. dry ther- mometer (°C) | Temp. wet thermom. (°C) | Relative humidity | |
|------------------------|---|------------------------------------|----------------------|--|
| 0 | RT | -- | -- | Stored |
| 0,25 | + 40 | 36,5 | 80 | Ideal value reached |
| 25 | + 40 | 36,5 | 80 | New ideal value set |
| 25,75 | - 30 | -- | -- | Ideal value reached |
| 47,7 | - 30 | -- | -- | New ideal value set |
| 48,7 | + 40 | 36,5 | 80 | |
| 71,6 | + 40 | 36,5 | 80 | New ideal value set |
| 72,3 | - 30 | -- | -- | |
| 95,8 | - 30 | -- | -- | Simulation finished, specimen stored. |

5.32 Thermal vacuum

Length 210 hours, Temperature 180°C

Pressure 10^{-6} torrs

The modules showed no mechanical or visual changes after the test. The electrical properties and the weight also remained practically unchanged:

First module:

Before the test: $I_K = 232 \text{ mA}$, $U_L = 1,134 \text{ V}$, $G = 5.0358 \text{ g}$

After the test: $I_K = 227.4 \text{ mA}$, $U_L = 1.149 \text{ V}$, $G = 5.0350 \text{ g}$

Second module:

Before the test: $I_K = 171.8 \text{ mA}$, $U_L = 1.134 \text{ V}$, $G = 5.9394 \text{ g}$

After the test: $I_K = 173.6 \text{ mA}$, $U_L = 1.116 \text{ V}$, $G = 5.0386 \text{ g}$

5.33 Thermal Shock

The test was accomplished by submerging the sample in liquid nitrogen (-196°C) and, after temperature adjustment, directly in water at $+80^{\circ}\text{C}$. After 20 temperature cycles the model showed no mechanical or visual changes. Changes in the electrical properties also are inside the region of measurement error:

Before the test: $I_K = 219.9\text{ mA}$, $U_L = 1.134\text{ V}$

After the test: $I_K = 218.6\text{ mA}$, $U_L = 1.131\text{ V}$

5.34 Vibration

A test module was loaded in the z-direction (perpendicular to the module surface), a- and b- directions (parallel to the module sides) with sine and random vibration according to the specifications:
a) sine oscillations, 2 octaves/min, always $\frac{1}{2}$ cycle with 2 octaves/min.

z-axis: from 10 - 67 H_2 with $\pm 2.5\text{ g}$

67 - 100 H_2 with 15 g

100 - 500 H_2 with 22.5 g

500-2000 H_2 with 7.5 g

a- and b- axes, each time from 5 - 13 Hz with $\pm 6.85\text{ g}$

13 - 400 Hz with 4.5 g

400 - 2000 Hz with 7.5 g

b) random vibration, $0.07\text{ h}^2/\text{H}_2$ power density, a-, b-, and z- axes, each for 4 minutes in the frequency band

20 -2000 Hz with 11.8 grms.

The module showed neither mechanical, visual, electrical, nor any kind of changes:

Before the test: $I_K = 241.9 \text{ mA}$, $U_L = 1.146 \text{ V}$

After the test: $I_K = 241.9 \text{ mA}$, $U_L = 1.142 \text{ V}$

6. INVESTIGATIONS ON THERMAL BALANCE

6.1 Test Module

a) Module with 2 solar cells and 2 second surface mirrors (55 m of 150μ quartz/silver of $2 \times 2 \text{ cm}$) see Figure 28. The fabrication was shown in 5.2 (but without electrical connector) with additional blackening of the module back side (black lacquer type PT-404A high heat coating). The second surface mirrors are described in Ref. 3.

b) Module with 4 solar cells, see Figure 27. The fabrication proceeded as described in 5.2 (but without electrical cell connector) with additional blackening of the back side of the module (black lacquer type PT-404A high heat coating).

A thermoelement (copper-constantan, 0.2 mm wires) was welded to the front side of the module (on the grid strand of one of the four cells, a second was bonded to the back side of the module (i.e., to the Mg alloy sheet). Connections were made on one cell to measure the short-circuit current and no-load potential during the tests.

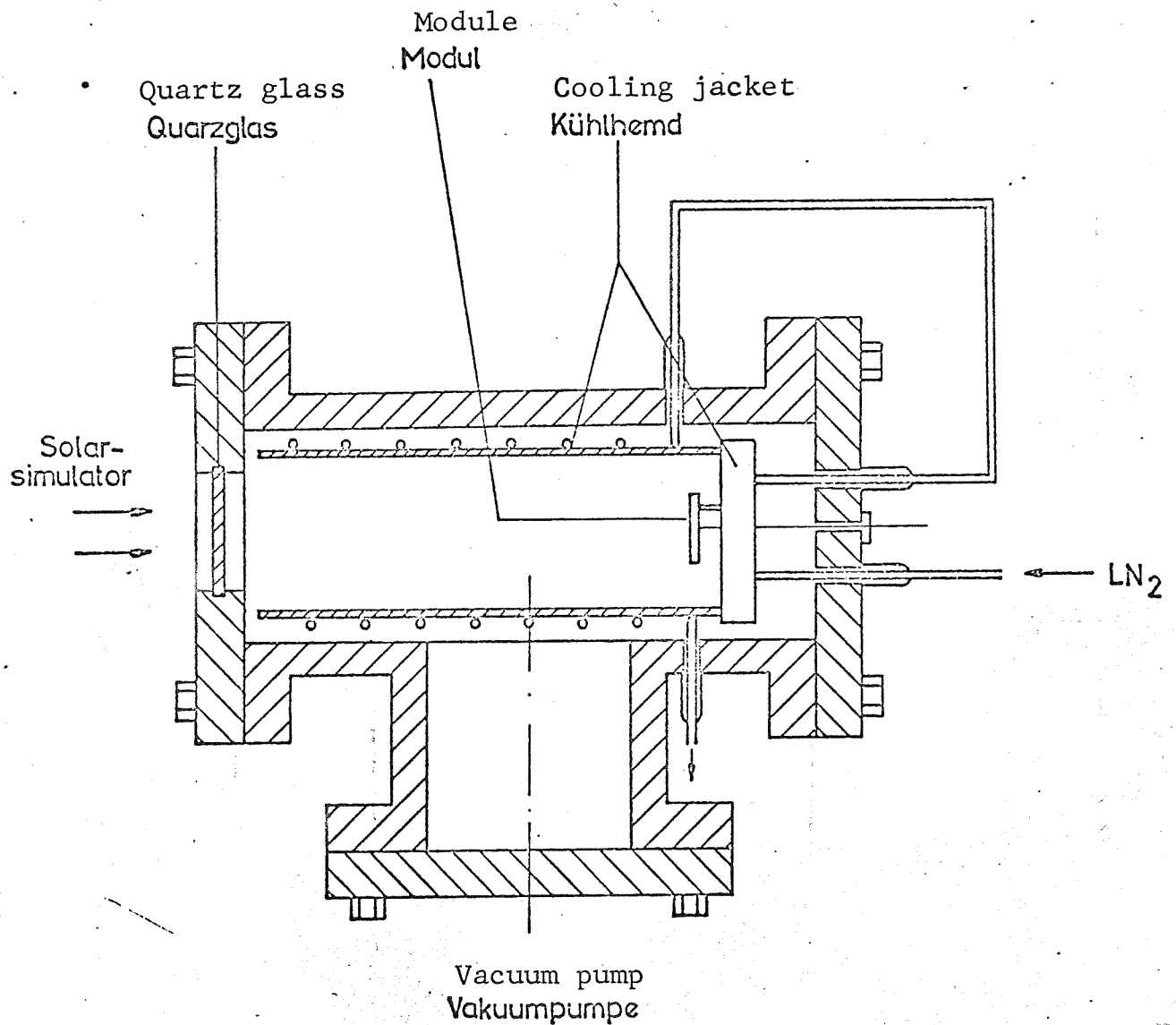
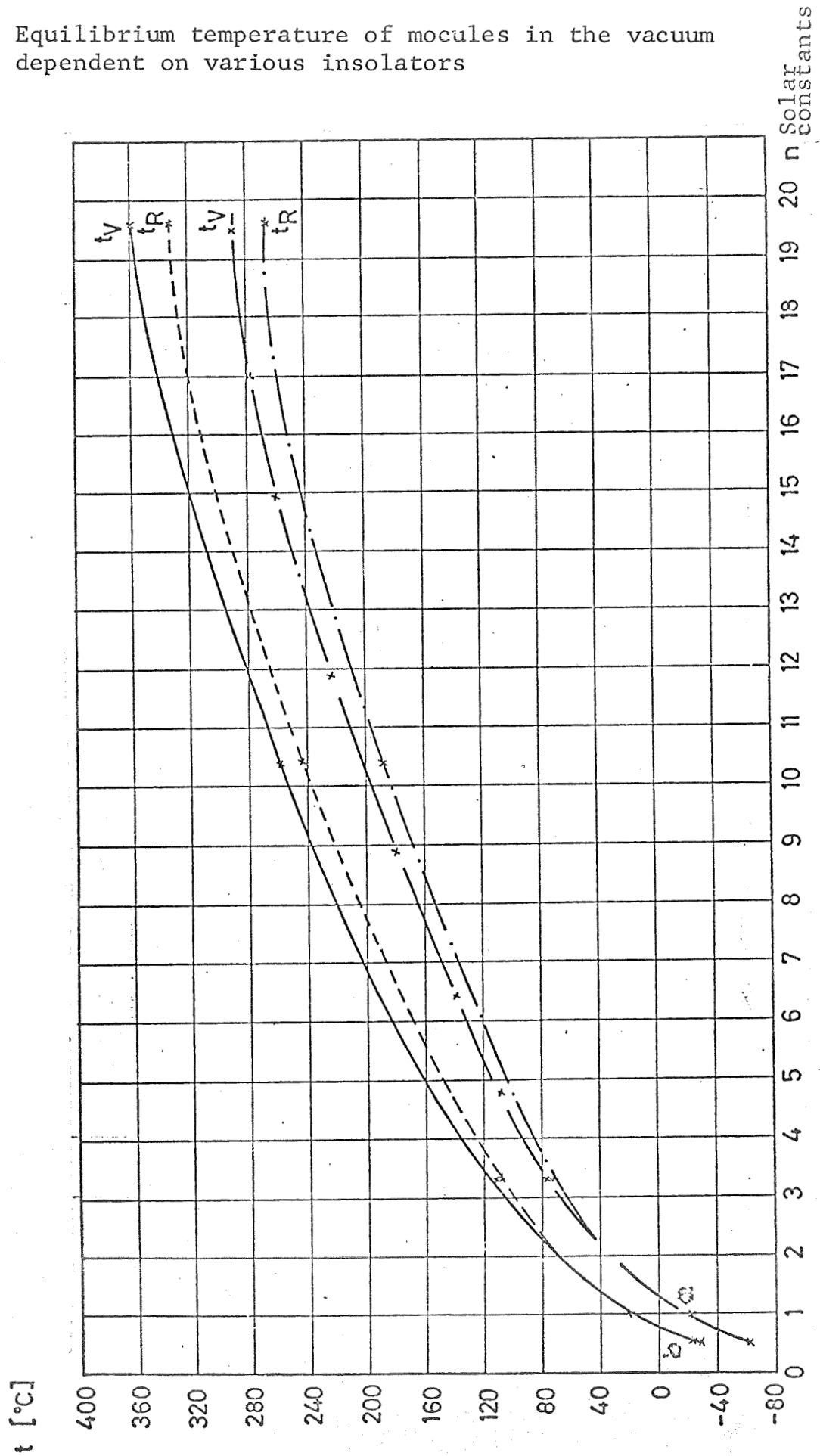


Figure 30 Schematic of the test chamber

Figure 31 Equilibrium temperature of mocules in the vacuum dependent on various insulators

Diagram: Heat balance $t = f(n \cdot SK)$

$$n = \frac{\text{measured short-circuit current}}{\text{short-circuit current at 1 SC}}$$



6.2 Test Setup

The modules were built into a vacuum chamber (Figures 29, 30) and isolated from the heat. The electrical leads for cells and thermoelements were vacuum sealed and led outward. Behind the module and to the side was a blackened LN_2 cooling jacket. The high solar constants were produced by a xenon high pressure lamp (6.5 KW) from the Osram Company and a Bosch solar simulator (cf. Ref. 3). The matching of the xenon spectrum to the sun spectrum was attained with a suitable filter.

6.3 Calibration of the Solar Simulator

On the basis of previous tests (cf. Ref. 3) and chiefly for reasons of time the earlier calibration values were taken on. At the end of the tests a final calibration was undertaken with a calibration instrument finished at that time with a solar cell (type V) (especially for very high insulations) and the values used previously were corrected. The calibration for a solar constant was accomplished with a Heliothek calibration cell. By the proportionality of the short-circuit current of the solar cells used and the insolation, the size of the insolation could be measured accurately to ca. 5%.

6.4 Result

Table 21 and Figure 31 show the equilibrium temperatures

obtained for the various insulations from 0.5 to 19.6 solar constants. The temperature difference between the front and back side of the module ($T_V - T_R$) remained small. The size was small and increased with the temperature. It was determined as follows:

In the heat equilibrium (ignoring the radiation from LN₂ ambient temperature):

whereby α = Absorption capacity of the module front side
(for solar light)

ϵ_V = Emission capability of the module frontside
(thermal radiation)

ϵ_R = Emission capability of the module back side
(thermal radiation)

T_V = Temperature of the module front side

T_R = Temperature of the module back side

$\sigma = 5.67 \cdot 10^{-12} \text{ W/cm}^2 \text{ } ^\circ\text{K}^4$ (Boltzmann's radiation constant)

$S_0 = 0.140 \text{ W/cm}^2$ (solar constant)

n = number of radiating solar constants

with $T = \frac{T_V + T_R}{2}$ one obtains approximately

$$\frac{\sigma T^4}{n S_0} = \alpha / (\epsilon_V + \epsilon_R) = 4,05 \cdot 10^{-11} \frac{T^4}{n};$$

with $\bar{\epsilon} = \frac{\epsilon_V + \epsilon_R}{2}$

$$\text{then } \frac{\alpha}{\bar{\epsilon}} = 8,1 \cdot 10^{-11} \frac{T^4}{n}.$$

For the pure solar cell module one obtains, according to Table 21, $\frac{\alpha}{\bar{\epsilon}} \approx 0.6$. Since for pure second surface mirrors $\frac{\alpha}{\bar{\epsilon}} \approx 0.1$

a value of $\frac{\alpha}{\epsilon} \approx \frac{0.6 \times 0.1}{2} = 0.35$ is to be expected for the mixed module, whereby the result of Table 21 is consistent.

Basically, one can say that the $\frac{\alpha}{\epsilon}$ values of a module and, thus, the equilibrium temperatures are dependent on the cleanness of the SSM (no adhesive remnants after the assembly!), the heat transfer resistivities between cell or SSM and the carrier sheet, the distance between cell and SSM ($\frac{\alpha}{\epsilon} = 1$ for evacuated spaces!) and, naturally, the relationship of the surfaces covered with the SSM and the surfaces covered with solar cells. All these parameters can be experimentally changed and refined. With the technique used here for the construction of mixed modules, it is already possible to keep the temperature under 200° C in an insolation of 10 solar constants (cf. Table 21). Of course, the selected distribution of cells and SSM's in the thermal limiting conditions does not correspond to any section of solar cell panel. Further studies are necessary for this.

TABLE 21

Measurement Values for the Thermal Balance Tests

| t_V °C | t_R °C | T_V °K | T_R °K | $\frac{T_V - T_R}{2}$ | $T \cdot 10^8$ | $\frac{\alpha}{\epsilon}$ | n (sk) | Comments |
|-------------|-------------|-------------|-------------|-----------------------|----------------|---------------------------|--------|--------------------------|
| -29 | -26 | 244 | 247 | 245,5 | 36 | 0,582 | 0,5 | Module without SSM |
| +20 | +20 | 293 | 293 | 293 | 73,6 | 0,543 | 1,1 | |
| 114 | 110 | 387 | 383 | 385 | 219,2 | 0,538 | 3,3 | |
| 258 | 245 | 531 | 518 | 524,5 | 754 | 0,586 | 10,4 | |
| 361 | 336 | 634 | 609 | 621,5 | 1490 | 0,615 | 19,6 | |
| -62 | -59 | 211 | 214 | 212,5 | 20,23 | 0,33 | 0,5 | Module with SSM |
| -12 | -13 | 261 | 260 | 260,5 | 46,1 | 0,339 | 1,1 | |
| 79 | 72 | 352 | 345 | 348,5 | 146,4 | 0,359 | 3,3 | |
| 202 | 188 | 475 | 461 | 468 | 482 | 0,375 | 10,4 | |
| 290 | 268 | 563 | 541 | 552 | 925 | 0,382 | 19,6 | |

REFERENCES

- [1] B.R. Garrett, G.F. Blank, A.J. Ranadive
Broad Applications of Diffusion Bonding
NASA CR-409

- [2] D.R. Clarke (Boeing Company)
Thermal Annealing Solar Panel
Presented at Conference on Physics and Application
of Silicon (Lithium) Semiconductors
NASA (Goddard - Greenbelt Maryland, April 25, 1968)

- [3] Messerschmitt - Bölkow
Study on Coatings under Simulated Environmental
Conditions, Report No. TSR-6.428.1, Jan. 1969
(Experimental study under contract from the
Federal Ministry for Scientific Research)